Review

Air-Coupled Ultrasound Systems for Biomedical Applications: Advances in Sensors, Electronic Interfaces and Signal Processing Strategies

Filippo Laganà †, Riccardo Olivieri †, Elena Stuppia, Gianluca Barile, Giuseppe Ferri *, Salvatore A. Pullano

Posted Date: 2 February 2026

doi: 10.20944/preprints202602.0014.v1

Keywords: air-coupled; ultrasonic transducer; MEMS; biomedical sensing; time-of-flight; signal processing; AI-assisted analysis; electronic interface; ferroelectric; low-noise circuit

Review

Air-Coupled Ultrasound Systems for Biomedical Applications: Advances in Sensors, Electronic Interfaces and Signal Processing Strategies

Filippo Laganà [1,†], Riccardo Olivieri [2,†], Elena Stuppia [1], Gianluca Barile [2], Giuseppe Ferri [2,*] and Salvatore A. Pullano [1]

[1] Laboratory of Biomedical Applications Technologies and Sensors (BATS Lab), Department of Health Sciences, Magna Græcia University, 88100 Catanzaro, Italy

[2] Department of Industrial and Information Engineering and Economics, University of L'Aquila, 67100 L'Aquila, AQ, Italy

* Correspondence: giuseppe.ferri@univaq.it

† These authors contributed equally to this work.

Abstract

Air-coupled ultrasound (ACU) is emerging as a fully non-contact sensing modality in biomedical applications. ACU applications can be broadly classified into two main domains: (i) contactless monitoring of physiological parameters and (ii) assistive aids, robotic perception in unstructured real-world environments, enabling tracking and geometric reconstruction. Advances in electronic materials and sensors design have enhanced ultrasonic sensors characteristics (e.g. bandwidth, directivity, and intensity). In parallel, progress in front-end electronics and signal processing, including artificial intelligence (AI)-assisted analysis, has enhanced ACU performance under low signal-to-noise (SNR) conditions. This review focuses on low-frequency ACU systems, with emphasis on sensor technologies, electronic interfaces, and system architectures that enable non-contact biomedical and robotic applications.

Keywords: air-coupled; ultrasonic transducer; MEMS; biomedical sensing; time-of-flight; signal processing; AI-assisted analysis; electronic interface; ferroelectric; low-noise circuit

1. Introduction

Air-coupled ultrasound (ACU) technology has advanced substantially in recent years and is increasingly recognized as a promising contactless modality in medical applications, alongside optical and radio-frequency approaches [1–4]. ACU enables monitoring of physiological activity by sensing subtle body-surface vibrations and micro-displacements related to respiration and cardiac motion, supporting unobtrusive vital-sign tracking and biomechanical assessment [4–7]. It also contributes to medical and assistive robotics by enabling contactless ranging, target tracking, and geometric/anthropometric reconstruction in unstructured environment [8].

Although optical and radio-frequency methods can offer higher spatial resolution, they may be more sensitive to obstructions, lighting conditions, and privacy concerns [3,4]. Considering that airborne ultrasound sensing is bio-inspired, mammalian echolocation provides a natural paradigm for contactless ranging and sensing. Low-frequency ACU systems typically operate in the 20–100 kHz band, corresponding to millimeter-scale wavelengths, and can achieve sensing distances of up to a few meters [8–10]. Unlike contact ultrasound, ACU operates without coupling media, enabling measurements and interaction in scenarios where contact is impractical, undesirable, or unreliable [11]. Despite focusing on different application scenarios, biomedical and robotic sensing share similarities in sensing principles and architecture, electronic interfaces, and algorithms [12,13]. These applications share a common technological challenge: achieving adequate bandwidth, directivity,

 doi:10.20944/preprints202602.0014.v1

and acoustic output in air [14]. Emerging trends are also evident in multimodal sensing, where ACU is combined with optical or inertial technologies [15]. Furthermore, data-driven processing techniques, such as AI-assisted micro-movement extraction, can further improve the system's robustness and real-world applicability [16].

Advances in ACU has been closely tied to development in sensor technologies, including piezoceramics, ferroelectric polymers and micro-electro-mechanical systems/micro-machined ultrasonic transducer (MEMS/MUT) sensors, together with dedicated front-end electronics for excitation, impedance matching, and low-noise signal acquisition [17–19]. Piezoceramic transducers are widely used in air-coupled applications due to their high electromechanical coupling and robustness, enabling the generation of ultrasonic waves with sufficiently acoustic pressure despite the strong acoustic-impedance mismatch with air [20,21]. In parallel, MUTs are increasingly adopted for air-coupled systems because their multichannel array architectures support advanced beamforming and acoustic imaging, which are particularly relevant for medical and assistive robotics under occlusions, variable lighting, and privacy constraints [22,23]. Finally, ferroelectric polymers such as polyvinylidene-fluoride (PVDF) and its copolymers (e.g., P(VDF–TrFE)) are attracting interest for airborne operation because their acoustic impedance is closer to that of air than conventional piezoceramics, potentially improving transmission efficiency and reception sensitivity [18,24]. Recent work suggests that such ferroelectric in membrane or planar array configurations can enhance acoustic coupling in air and provide high fractional bandwidths, supporting the detection of physiological micro-movements and contactless perception tasks [24,25]. Despite progress in transducer design, air propagation remains fundamentally constrained by frequency-dependent attenuation, sensitivity to temperature and humidity, and pulse dispersion, resulting in an inherent trade-off between spatial resolution and operational range [26–28]. In this context, the design of dedicated electronic front ends is critical to preserve weak echo signals and maximize system sensitivity under low signal-to-noise ratio (SNR) conditions. Advances in conditioning circuits and synchronized multi-channel architectures have partially mitigated these limitations, improving scalability and robustness [29]. Finally, modern ACU systems increasingly rely on advanced signal processing and knowledge-driven algorithms to extract reliable information from highly attenuated and noisy ultrasonic signals in realistic biomedical and robotic environments [30,31].

This review will focus ACU with emphasis on sensor technologies, front-end electronic interfaces, and system-level architectures that enable robust and scalable solutions for biomedical monitoring and medical/assistive robotics.

2. Air-Coupled Ultrasound Sensing

2.1. Generation and Reception of Low Frequency Ultrasound

Air-coupled ultrasound relies on the transmission of acoustic waves through air, a medium whose acoustic impedance is several orders of magnitude lower than that of other media (e.g. biological tissues, and most solids) [32]. This extreme mismatch is the primary physical constraint of airborne ultrasonics and leads to acoustic reflection at air–solid interfaces [17–19]. Ultrasonic propagation in air is strongly affected by frequency-dependent attenuation (which increases at higher frequencies), dispersion, and environmental factors such as temperature and air currents [33]. Figure 1a schematically shows the ACU operating principles and the main physical factors that limit pulse transmission and echo reception in air (high attenuation, impedance mismatch, scattering, and environmental effects). Although ACU has been explored across a broad frequency range, practical operation for biomedical sensing and field deployment is typically pushed toward low frequencies, often < 100 kHz, because sound attenuation in air increases strongly with frequency (commonly approximated as $\alpha \propto f^2$) [32,33]. A typical ACU chain starts with signal generation via pulsed, burst, or coded excitation of a transmitting (TX) element (Figure 1b). In air, the average sound speed is about 343 $m \cdot s^{-1}$ at 20 °C and shows a temperature dependence of roughly 0.6 $m \cdot s^{-1} \cdot °C^{-1}$, which must be compensated to ensure accurate pulse-echo timing estimation (e.g. time-of-flight, TOF) [34,35]. Weak

 doi:10.20944/preprints202602.0014.v1

echoes are converted back to electrical signals by a receiving (RX) element and conditioned through high-impedance, low-noise preamplification and band-limited filtering prior to digitization and processing (Figure 1b) [36]. Since coupling losses at the transducer–air boundary dominates airborne operation, acoustic matching layers with intermediate impedance are frequently adopted. For a single matching layer, the optimal impedance is commonly expressed as $Z_{layer}=\sqrt{(Z_{material}\, Z_{air})}$ [37]. Lightweight polymeric layers are therefore attractive, and electrets (charged porous cellular polymers exhibiting piezoelectric characteristics) have emerged as effective candidates to support more efficient air coupling [38,39].

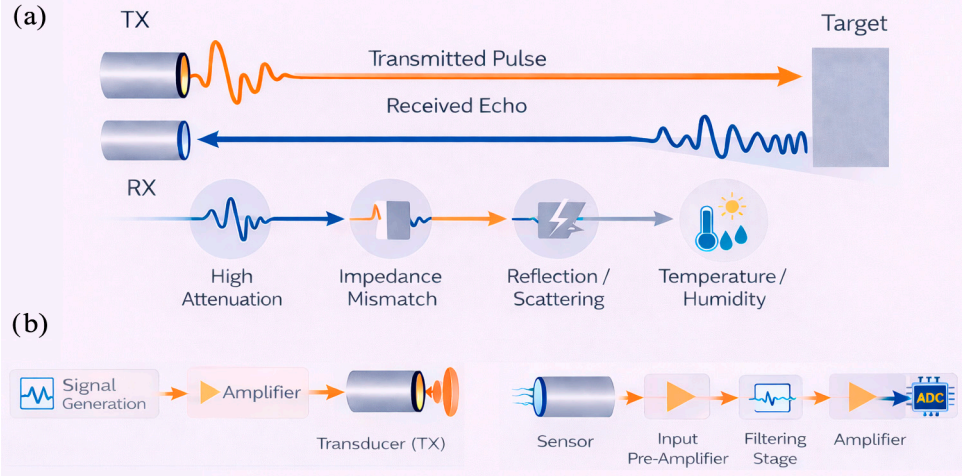

Figure 1. (a) Low-frequency ACU pulse transmission and echo reception in air, highlighting key limitations: high attenuation, impedance mismatch, reflection/scattering, and temperature/humidity effects. (b) Typical ACU architecture: transmit chain (signal generation and power amplification driving the TX transducer) and receive chain (sensor, pre-amplification, filtering, amplification, and downstream digitization/signal processing).

In ACU, excitation is typically tailored in terms of duration, spectral content, and modulation. In biomedical/field ACU systems, carrier frequencies are often in the 20–100 kHz range (most frequently 40 kHz) [2,10]. Constant-frequency (CF) excitation includes continuous-wave tones transmitted over long intervals (tens to hundreds of ms, or longer). CF is well suited for phase/Doppler tracking (sub-mm motion) but provides limited range discrimination alone [6,40]. Short tone-bursts gate the same carrier over a few to tens of cycles. Typical bursts use ~5–20 cycles, i.e., ~0.1–0.5 ms at 40 kHz. Burst length trades energy/SNR against temporal resolution and echo overlap [8,32]. Broadband transients are obtained by very short pulses or click-like waveforms. Impulse-like drives may be ~1–3 effective cycles (≈25–75 μs at 40 kHz), sharpening TOF localization [7,8]. Their effective bandwidth can reach several tens of kHz but is limited by the transducer and filtering [18,20]. Frequency-modulated (FM) signals sweep across a band (linear or non-linear chirps) [28]. Practical sweeps may span, for example, 30–90 kHz over ~1–5 ms. Such sweeps inject more energy without increasing peak pressure, thereby improving detectability in air. Matched filtering/pulse compression is used to recover a short effective echo response [10,26]. Waveform selection is a system-level choice balancing coupling losses, SNR, motion tolerance, and timing accuracy [11,21].

2.2. ACU Application in Physiological Monitoring and Medical Robotics

Low-frequency ACU systems are typically deployed with different operating modes depending on whether the target application is (i) contactless physiological monitoring or (ii) robotic perception in unstructured real-world environments, enabling tracking and geometric reconstruction (see Figure 2a).

 doi:10.20944/preprints202602.0014.v1

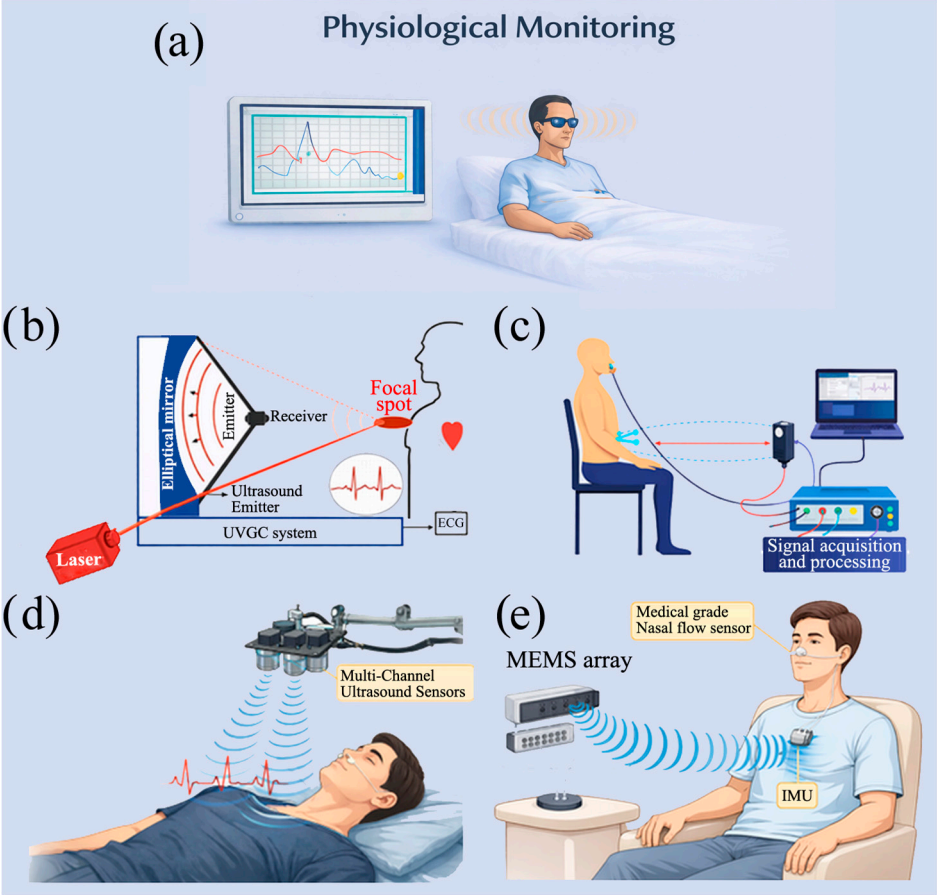

Figure 2. (a) Contactless physiological monitoring, where airborne ultrasound tracks subtle body-surface vibrations associated with respiration and cardiac activity without physical contact. (b) Non-contact and through-clothing measurement of the heart rate (HR) using ultrasound vibrocardiography (adapted from [40]). (c) Noncontact respiration rate measurement system using an ultrasonic proximity sensor (adapted from [46]). (d) Multi-channel ultrasound system for non-contact heart rate monitoring (adapted from [42]). (e) System for contactless respiratory waveform estimation using ultrasound planar array adapted from [41]).

In physiological monitoring, ACU is primarily used to capture subtle body-surface vibrations and micro-displacements associated with respiration and, in more demanding settings, cardio-mechanical activity [4,5]. The interest in ACU systems lies in the possibility of performing prolonged, non-invasive measurements in sensitive contexts, such as home monitoring, intensive care units and situations where physical contact with the patient is critical or undesirable. In such scenarios, the robustness and stability of the system over time become as important as, if not more important than, spatial resolution.

Representative implementations commonly operate at 40 kHz and adopt a single-view ranging configuration in which a transmitter irradiates the thorax/upper-body region and a receiver collects the reflected field, enabling respiration monitoring in bed-like conditions and other unobtrusive scenarios [4–7]. In this domain, performance is rarely limited by spatial resolution; rather, the key requirements are coherent detection, high receive sensitivity, and robustness under low SNR. Accordingly, the signal-processing focus is on extracting quasi-periodic motion rather than forming detailed images. Signal processing strategies typically include: (a) repeated TOF tracking to follow slow range changes over time, (b) phase and/or amplitude demodulation to enhance sensitivity to sub-millimetric motion, and (c) frequency-domain analysis (FFT or time–frequency features) to estimate respiratory rate and related descriptors from the motion signal.

Phase-based approaches have been explicitly adopted to increase sensitivity in cost-effective air-coupled breathing systems. In support of the above considerations, there have been experimental studies showing the feasibility of ACU systems in the field of non-contact physiological

 doi:10.20944/preprints202602.0014.v1

measurements. These studies provide concrete validation of signal acquisition and processing strategies, demonstrating that micro-vibrations and micro-displacements on the surface of the human body can be reliably detected without mechanical coupling with the subject. One of the most representative contributions is [40], where cardiac activity is estimated by analysing the phase modulation of the reflected ultrasonic signal, which is induced by the heartbeat on the chest wall, even under the presence of clothing (see Figure 2b). The main strength of this approach is the complete absence of physical contact, making it very suited to unobtrusive long-term observation settings. However, the study also mentions the natural limitations of this method as having a high sensitivity to gross subject movement and an incomplete characterisation of the electronic front-end parameters. To improve measurement robustness, a multi-channel acquisition architecture is introduced, allowing the signal-to-noise ratio to be increased through the spatial combination of Doppler signals (see Figure 2c) [41]. This strategy improves stability and reliability under low SNR conditions, but at the cost of increased hardware complexity and power consumption, which are critical constraints for embedded and portable applications. An alternative approach, characterised by greater architectural simplicity, is proposed in [42], where heart rate estimation is based on the periodicity of Doppler frequency variations with reduced hardware. However, the strong dependence on the geometric stability of the measurement setup limits its reliability in uncontrolled contexts. A particularly significant contribution is represented by [43], which demonstrates the possibility of simultaneously extracting cardio mechanical and respiratory information from a single ACU sensor. The major strength of this study lies in its high level of functional integration, whereas the lack of a systematic discussion on filter design and spectral separation of physiological components can be seen as a limitation in methodology. Non-contact respiratory monitoring has been extensively explored in studies such as [44,45]. In these studies, respiration is estimated by analysing slow variations in distance or phase of the reflected ultrasonic signal. These approaches have the advantage of low cost and easy implementation but suffer from limited temporal resolution and sensitivity, with performance highly dependent on post-processing techniques. More advanced configurations, such as [46], demonstrate that the use of air-coupled ultrasonic arrays allows the entire respiratory waveform to be reconstructed, improving the temporal continuity of physiological information (see Figure 2d, 2e).

However, this improvement comes at the cost of greater hardware and computational complexity.

Subsequent studies have extended the non-contact ACU techniques to enable the simultaneous analysis of multiple human body parameters, thus reducing sensitivity to operating conditions and improving overall robustness. In reference [47], a joint phase Doppler system is presented for estimating cardiac and respiratory information simultaneously, with greater stability than those that utilise different domains. Similarly, reference [48] illustrates that vital information can be obtained by combining the time of flight and phase variations. An approach specifically orientated towards Doppler-based respiratory monitoring is presented in [49], where respiration is estimated from thoracic micro-oscillations induced by the respiratory cycle. Although the architecture is simple and low-cost, performance is highly dependent on the geometry of the setup and the orientation of the sensor [50–54]. A comparative summary of the main non-contact ACU studies for physiological monitoring, including the stated acquisition parameters where available, is shown in Table 1.

Table 1. Contactless ACU studies for physiological monitoring

Application	Operating Mode	Transducers (Material/Type)	Frequency range (kHz)	Bandwidth	Sensitivity	SPL	Electronic Interfaces	Ref.
Vibrocardiography (HR)	Pulse-Wave Doppler	PZT 20-1330 (APC International Ltd) transducer + ultrasonic microphone FG-	20-60 (operating frequency), 50 (carrier	20-60 kHz (Emission - reception system),	-53 dB	N/A	Agilent U2542A DAQ + microphone,	[40]

 doi:10.20944/preprints202602.0014.v1

		23329, Knowles Electronics receiver	frequency PW Doppler)	10-100 kHz (electronic preamplifier)			preamplifier	
Respiratory Rate Monitoring	TOF	UNDK 20U6903 ultrasonic proximity sensor (Integrated Tx/Rx)	240 (proximity sensor)	N/A	N/A	N/A	0-10 V DC analog output+ BIOPAC MP150 DAQ	[46]
Respiratory Waveform Estimation	Pulsed excitation: pulsed Doppler; FMCW: FMCW Doppler	Emitter: 5 W speaker; Receiver: 4x4 MEMS array (UMA-16, SPH1668LM4H)	Pulsed: 18; FMCW: 16.8-20.8; Beamforming pulses: 8	4 kHz (16.8-20.8 kHz)	-29 dB	N/A	Microphone array + amplification + ADC (44.1 kHz) + digital processing	[41]
Heart rate and heart rate variability (HRV)	Air-ultrasound transducer + motion tracking	MCUSD40A100 B17RS	~100	N/A	N/A	N/A	GRAS™ 12AA 2-channel power module	[43]
Chest vibrometry (RR)	TOF /phase-delay; cross-correlation of successive echoes, measuring surface normal velocity	Emitter:37 piezoelectric diaphragms (Murata 7BB-20-6), used all in parallel for ultrasonic emission, Receiver: 6 high-frequency microphones (Knowles FG-23329) connected in parallel	20-60	40 kHz	-53 dB each	N/A	Piezoelectric array driven by single electronic amplifier (emission) + microphone signal 40 dB amplified, analog front-end+ Agilent U2542A DAQ	[6]
Multi-channel ultrasound system for HR monitoring	CW ultrasound Doppler (phase-based)	Piezoelectric US (SensComp 40LT16 transmitter / 40 LR 16 receiver)	40	2 @ -6 dB	-65 dB	120 dB min	VCO + phase detector (XOR) + LPF + ADC	[46]
Air-ultrasound skin motion HR/HRV	TOF air-ultrasound distance measurement	Air-coupled piezoelectric ultrasound transducers (Multicomp Pro MCUSD40A100 B17RS)	100 (operating frequency), 95-105 (chirped excitation)	89-111 kHz (transducer bandwidth, 22 kHz (-6 dB electroacoustic response)	N/A	N/A	High-voltage waveform generator, impedance matching circuit, air-ultrasound transceiver, digitizer	[50]

In robotics and assistive technologies, ACU can support ranging, obstacle detection, target tracking, and coarse geometric reconstruction when optical sensing is degraded by occlusions, variable illumination, specular/transparent surfaces, or privacy constraints. In this environment, the emphasis shifts from maximizing sensitivity to periodic micro-motion toward reliable TOF estimation, adequate spatial coverage, and robustness to multipath and surface-dependent reflectivity (see Figure 3a). Biomimetic and sonar-inspired lines of work have demonstrated how

 doi:10.20944/preprints202602.0014.v1

engineered reflectors/beacons and acoustic cues can support navigation and localization performance in cluttered scenes, motivating designs that explicitly manage echo structure.

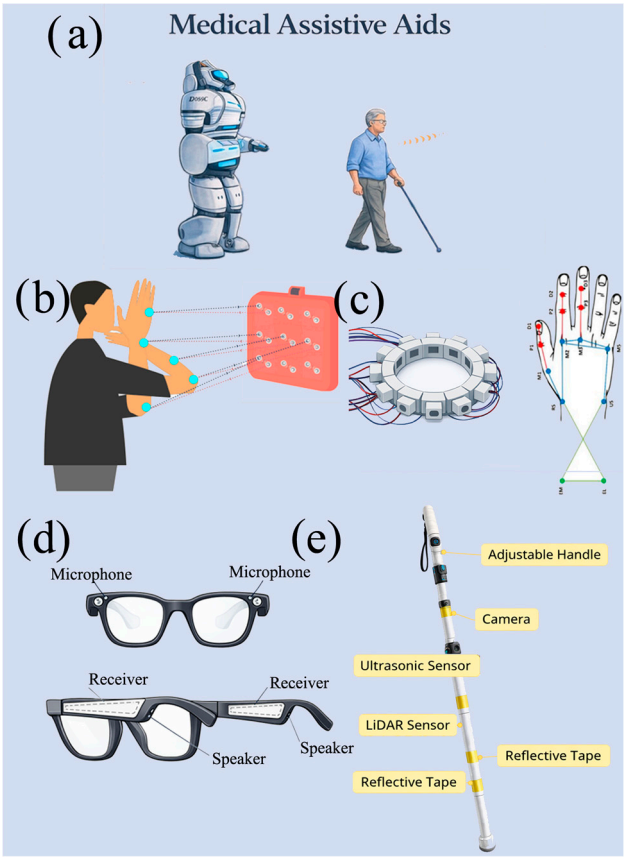

Figure 3. (a) Ultrasonic assistive aids and medical robotics, including obstacle detection and navigation in unstructured environments using biosonar-inspired time-of-flight sensing, applied to devices such as smart canes, wearable sensors, and mobile assistive aids. (b). Ultrasound-based gesture recognition contactless system (adapted from [55]). (c) Wearable ultrasound (bracelet) for wrist and hand kinematic tracking (adapted from [56]). (d) Smart glasses with integrated left/right microphones, receivers, and speakers adapted from [57,58]). (e) Smart cane with integrated sensing modules and user-feedback elements (adapted from [59,60]).

Assistive navigation devices represent a pragmatic instance of this operating mode: "smart cane" concepts leverage ultrasonic time-of-flight distance sensing to alert users to obstacles, with recent designs emphasizing usability and operation across diverse conditions. In medical and assistive robotics, similar sensing principles can be integrated on mobile platforms to provide short-range perception in patient-facing environments, where conservative sensing (e.g., presence/distance) may be preferred over imaging for simplicity and privacy.

In addition to vital-sign monitoring, ACU sensors have been used for the quantitative assessment of human movement, with particular relevance to neurological and rehabilitation (see Figure 3b). In [55], repetitive finger movement is quantified by analysing variations in the flight time of the ultrasonic signal. A key advantage of this approach is its high sensitivity to micro-movements, which makes it particularly suitable for screening motor disorders. However, the limited measurement range and the need for accurate sensor alignment represent significant application constraints. Extensions to hand and gesture tracking are discussed in [26,61,62]. These studies show how the absence of wearable sensors improves user acceptability, but at the cost of lower spatial resolution compared to vision-based systems and greater sensitivity to environmental reflections. Subsequent studies have shown that the accuracy of motion detection can be further improved by analysing micro-variations in the phase of the ultrasonic signal. In [63], the possibility of detecting micro-movements of the limbs with sub-millimetre resolution is demonstrated, making the approach

 doi:10.20944/preprints202602.0014.v1

particularly promising for neuromotor monitoring applications. A further extension is proposed in [59], where a hybrid strategy based on time-of-flight and Doppler allows dynamic tracking of fingers and hands, improving the temporal continuity of the signal compared to single-domain solutions (see Figure 3c) [55]. Beyond biomedical monitoring, ACU has also been successfully integrated into assistive technologies for users with visually impaired (see Figure 3d) [56,57]. For example, ultrasonic smart eyeglasses employ frequency modulation/demodulation to sense obstacles in both indoor and outdoor environments, providing real-time spatial cues without requiring direct contact. Another assistive application is the electronic cane equipped with ACU transducers (see Figure 3e) [57,60] which exploit TOF measurements to identify hazards ahead of the user. These devices demonstrate how ACU systems can be effectively integrated into mobility aids for enhanced environmental perception. Solutions based on air-coupled ultrasonic arrays, such as [60], show that spatial localisation accuracy can be significantly improved through multi-channel acquisition and beamforming techniques. However, these benefits are accompanied by increased costs, size and power consumption, which can limit adoption in compact medical devices. An overview of representative studies dedicated to physiological and motor assessment using non-contact ACU sensors is shown in Table 2.

Table 2. Contactless ACU studies for physiological and motor applications

Application	Operating Mode	Transducers (Material/Type)	Frequency range (kHz)	Bandwidth	Sensitivity	SPL	Electronic Interfaces	Ref.
Hand gesture / person identification	Pulse-echo / time-of-flight	HC-SR04 ultrasonic distance sensor module	40	1-3 kHz	-65/-75 dB	110-120 dB	Arduino Mega 2560 + ATtiny85;	[55]
Human ultrasonic echolocation device	Pulsed Frequency-Modulated (FM) ultrasonic chirps	Ultrasonic loudspeaker (Tx) Fostex FT17H Realistic Super Tweeter + 2 Ultrasonic microphones (Rx, binaural) Bruel & Kjaer Type 4939 microphones	5-50	45 kHz	4 mV/Pa	98.5 dB/W	PC-based signal generation and processing (MATLAB) + Sound card ESI Juli@ (192 kHz I/O) + Power amplifier Lepai Tripath TA2020 + Microphone preamplifier B&K 2670 + B&K Nexus + Playback: Gigaport HD USB sound card + open-ear headphones	[62]
Obstacle detection for visually impaired (Assistive)	Pulsed ultrasonic TOF with phase-modulated pulse trains (DPSK); distance calculation via TOF + echo validation via phase-	2 x piezoelectric air-coupled ultrasonic transducers per sensor (1 Tx + 1 Rx), SRF08, HC-SR04	40	1-3 kHz	-65/-75 dB	110-120 dB	Ultrasonic module: HC-SR40 (modified) + microcontroller ATMega328P (Arduino Nano) + digital trigger / echo interface + on-board analog comparator and ADC for	[7]

 doi:10.20944/preprints202602.0014.v1

	code modulation						echo detection + Bluetooth module (HC-06) for data transmission to smartphone	
Smart glasses for blind people	Frequency modulation / demodulation	Omni-directional digital microphones (IMP34DT05TR)	20 up to 48	N/A	N/A	N/A; < 70 dB (environment)	Digital audio interface (PDM, I²S)	[57,60]
Smart cane	TOF	HC-SR04 ultrasonic transceiver	40	N/A	N/A	N/A	Digital I/O (TRIG/ECHO timing interface)	[58,59]

Studies confirm the potential of air-coupled ultrasonic sensors for non-contact biomedical sensing while also highlighting marked heterogeneity in system architectures and reporting practices. From a system perspective, these robotic operating modes more frequently benefit from synchronized multi-channel acquisition and, where available, array-based operation to improve directivity control, suppress spurious echoes, and stabilize tracking in dynamic scenes. However, current research has revealed that multi-channel arrays and beamforming techniques can significantly improve the ranging accuracy of the ACU system when operating in different environments. It is important to note the need for an integrated design of the electronics, sensors, and algorithm in achieving the highest possible accuracy for both healthcare and robotic applications [4–8]. In summary, ACU sensing is inherently constrained by airborne propagation physics, resulting in low signal amplitudes and environmental sensitivity. These limitations motivate a system-level optimization approach in which sensor technologies, electronic interfaces, and signal processing techniques are jointly designed to achieve robust performance in biomedical and robotic applications. Studies have shown that a biomedical application of ultrasound is echolocation to provide human users with environmental cues rich in objective and spatial information that are more elaborate than other assistive devices. The devices in question are equipped with wearable headset with an ultrasonic emitter and a microphone with an artificial earcup attached [53]. In nature, the most sophisticated echolocation abilities are found in some animals such as some species of bats, dolphins and whales. The basics of human echolocation, on the other hand, remain poorly characterized and most of the existing literature suggests that the human echolocation capacity does not come close to the precision and versatility found in highly specialized organisms. The ultrasonic pulses employed by echolocalized animals produce higher spatial resolution, stronger directionality, and higher bandwidth than human-audible frequencies. Inspired by the biological mechanism of bats and cetaceans, these systems rely on the deliberate emission of ultrasonic pulses – typically ranging from 20 kHz to 200 kHz and up to 2 MHz in case of high-resolution medical imaging – to map the environment and detect obstacles. The principle involves computing the TOF between the trigger of an ultrasonic burst and the reception of its reflected echo, a process that requires precise synchronization and specialized electronics stages [62]. Echolocation systems offer the possibility to acquire anatomical and biomechanical information from tissue without direct coupling, indicating potential for advanced biomedical localization and allowing the realization of assistive human echolocation devices.

3. Sensor Technologies

3.1. Sensors Design and Characterization

The characterization of air-coupled ultrasonic sensors relies on a combination of electrical, electromechanical, and acoustic parameters (e.g., resonance frequency, sound pressure level (SPL),

 doi:10.20944/preprints202602.0014.v1

receiving sensitivity, and spatial radiation), which represent the fundamental metrics for comparing different sensor technologies [66–70]. The resonance behavior of ultrasonic sensors is commonly analyzed using equivalent circuit models, such as the Butterworth–Van Dyke (BVD) model, which describes the electromechanical coupling through a resonant branch in parallel with static branch [69,70]. Experimentally, the complex input impedance or admittance of the transducer evaluated as a function of frequency. The resonance frequency is identified at the zero crossing of the imaginary part of the motional impedance, corresponding to the condition of purely resistive behavior [71,72]. From the frequency response, additional parameters such as motional resistance, capacitance, inductance, and quality factor can be extracted, providing insight into bandwidth and energy losses.

The acoustic output of an air-coupled ultrasonic transmitter is quantified in terms of sound pressure level. SPL measurements are performed at a fixed reference distance, typically 30 cm, under free-field or anechoic conditions [73]. The emitted pressure is expressed in decibels relative to the standard reference pressure of 20 μPa (see Figure 4a). Frequency-dependent SPL measurements allow the evaluation of transmission efficiency and usable bandwidth, which are critical in air due to strong frequency-dependent attenuation [74,75]. Receiving sensitivity is defined as the electrical output generated by the sensor in response to a known acoustic pressure [76]. Sensitivity is commonly expressed in Volt per Pascal (e.g., 10 V/Pa) or in decibel (see Figure 4b). Measurements are performed at the same reference distance used for SPL characterization to ensure consistency. Spatial characterization is carried out by measuring the angular dependence of the transmitted and received ultrasonic fields. Radiation patterns in transmission and sensitivity patterns in reception are typically acquired by rotating the sensor or the reference microphone over defined angular ranges on orthogonal planes (horizontal and vertical), see Figure 4c.

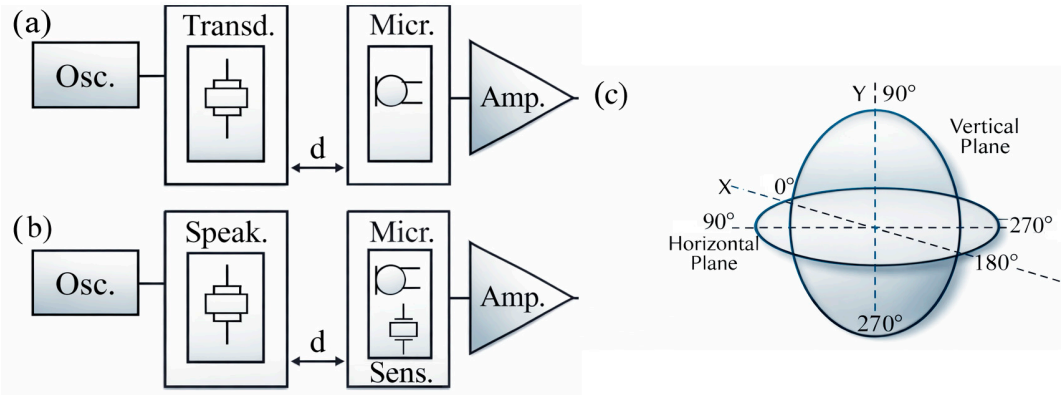

Figure 4. (a) Transmission–reception configuration used to characterize an ultrasonic transducer, consisting of a signal generator (oscillator), a piezoelectric transducer, a reference microphone placed at a fixed distance d, and a signal amplification and acquisition stage. (b) Measurement configuration employing a loudspeaker as acoustic source and a sensor under test as receiver, with the microphone used for reference calibration at distance d. (c) Definition of the angular reference system and measurement planes used for directivity and sensitivity characterization, showing horizontal and vertical planes (adapted from [75]).

Polar measurements yield beam-pattern diagrams that quantify beamwidth, directivity, and angular coverage, which are relevant for curved or non-uniform air-coupled ultrasonic geometries [77,78]. Since propagation in air is strongly affected by attenuation, dispersion, and environmental conditions (e.g., temperature and humidity) [79], sensor characterization is often complemented by system-level tests that assess the sensor together with the electronic interface and signal conditioning chain, providing a realistic estimate of sensitivity and signal-to-noise ratio [80].

 doi:10.20944/preprints202602.0014.v1

3.2. Sensors Materials

ACU transducers are typically fabricated using materials with either an acoustic impedance comparable with that of transmission medium or electromechanical properties capable of reducing the mismatch between transducers element and air [21]. The material most employed in ACU transducer de-sign include piezoceramics, piezoelectric composites, piezopolymers, polypropylene ferroelectret foams, silicone or silicone rubber combined with semiporous membranes and aerogels [81].

Table 3 summarizes the main material classes reported in the literature, along with their functional roles, advantages, and limitations.

Table 3. Material for ACU with their functional roles, advantages and limitations.

Material	Acoustic Characteristics	Advantages	Limitations	Ref.
PZT	High piezoelectric coefficients; acoustic impedance of 30-35 MRayl	Strong electromechanical coupling; efficient emission and reception; mature fabrication technology	Severe impedance mismatch with air; requires matching layers; narrow bandwidth	[34,35]
Composites PZT/polymer)	Acoustic impedance of 10-15 MRayl; enhanced compliance	Improved impedance matching in air, broader bandwidth; higher sensitivity in air	Lower mechanical robustness; more complex manufacturing	[27]
(PVDF)	Low acoustic impedance (3-4 MRayl); high piezoelectric flexibility	Lightweight, flexible, and suitable for abroad air coupling; good SNR when designed properly	Lower electromechanical coupling vs ceramics; higher electrical noise	[36]
Polypropylene Foams	Ultra-low acoustic impedance (0.05-0.1 MRayl); internal charged voids act as piezoelectric domains	Excellent acoustic matching to air; can act simultaneously as active transduction and matching layer; low mass	Limited power handling; potential aging of charged voids	[23,37]
Silicone Rubber Porous/Semiporous Membranes	Tuneable acoustic impedance via air filled microstructures; support half-wavelength cavity resonance	Enables highly efficient acoustic emission into air using resonance; adaptable to many transducer geometries	Narrowband response; sensitive to manufacturing tolerances	[23]
Aerogel	Extremely low density, acoustic impedance near air (0.02-0.03 MRayl)	Near-ideal impedance match; high transmission efficiency; emerging interest for broadband ACU	Fragile microstructure; challenging fabrication: moisture sensitivity	[35]
Silicone rubber	Reduced effective impedance due to micro voids	Improves transmissivity between transducer and air; simple and inexpensive	Limited bandwidth; material aging; strongly frequency-dependent	[82]

Among the most widely used materials are piezoelectric, which are sometimes combined with matching layers to better adapt the acoustic impedance between air and material, avoiding massive transmission losses [83]. Ultra-low impedance materials, such as ferroelectric foams and aerogels, have played a decisive role in mitigating the intrinsic misalignment between solid transducer

 doi:10.20944/preprints202602.0014.v1

elements and air, enabling broadband emission and significantly improved sensitivity compared to traditional piezoceramics. Recent studies further indicate that integrating ACU with computational imaging techniques — in particular with deep neural networks trained on spatiotemporal ultrasonic signatures — makes it possible to compensate for multipath propagation and atmospheric turbulence, significantly improving reconstruction quality in low SNR conditions typical of the air environment [84,85].

An example of a matching layer is based on epoxy resin filled with hollow polymer microspheres [86], which has a substantially lower acoustic impedance than piezoelectric materials (0.45 MRayl). Epoxy resin is also used combined with various fillers such as aluminium powder, aluminium-oxide (Al_2O_3) particles or tungsten powder [87]. In case of high temperature transducers, an organosilicon substrate is used as a single acoustic matching layer. Hollow glass microspheres (embedded in epoxy or organosilicon matrix) are used to obtain low-impedance matching [88]. To achieve a smooth transition between the high acoustic impedance of the transducer and the low impedance of the propagation medium, thus maximizing energy transfer over a wide range of frequencies, several different layers are also used together: for example, the aluminium alloy AlSi10Mg is used, which has an inherently high acoustic impedance (16.7 MRayl), and a standard epoxy resin that acts as a low impedance (2.7 MRayl) component (often used as a matrix polymer in contrast with high-impedance metal particles). The epoxy portion is dominant on the side that interfaces the air, and its percentage gradually decreases as it approaches the metal side of the alloy. This results in a continuous variation that ensures better acoustic transmission over broadband [89]. Ferroelectret materials are non-polarized dielectric polymers such as polypropylene (PP), polyethylene (PE), polyurethane (PU), Cyclo-Olefin Polymer (COP/COC), PTFE/FEP (fluoropolymers), polydimethylsiloxane (PDMS), and PVDF copolymers (with also a real ferroelectric component) [90]. They have a closed porous structure with smooth inner walls and features that make them better than classic ferroelectrics. Piezoelectricity comes from the deformation of pores, rather than from the movement of atomic dipoles as in ferroelectrics. They have a very high piezoelectric coefficient, very low dielectric permittivity, and are very light and flexible. The main advantage is the low acoustic impedance (≈ 0.03 MRayl), much closer to that of air [91]. The emergence of aerogel-based adaptation layers, whose acoustic impedance is close to that of air, has enabled near-ideal transmission characteristics, enabling broadband air sensing that was not achievable with conventional polymer interfaces.

3.3. Piezoceramic Sensor Design

Ultrasonic transducers based on piezoceramic materials, most commonly lead zirconate titanate (PZT), represent one of the earliest and most widely adopted solutions for air-coupled ultrasonic applications [88]. Owing to their high electromechanical coupling coefficients and mechanical robustness, PZT transducers are capable of generating high acoustic pressure levels in air. However, the large acoustic impedance mismatch between PZT ceramics (≈30 MRayl) and air (≈0.0004 MRayl) requires the use of dedicated mechanical and acoustic structures to ensure efficient sound radiation. To mitigate impedance mismatch, air-coupled PZT transducers are commonly implemented using horn-loaded architectures. In these designs, a thin or bulk PZT ceramic element is bonded to a mechanical horn that acts as an impedance transformer, progressively matching the high mechanical impedance of the ceramic to the low impedance of air [93].

Horn geometries are typically conical, exponential, or stepped, and are often combined with resonant cavities and dense backing materials to enhance forward radiation and suppress backward emission (see Figure 5).

The horn length is frequently designed according to a quarter-wavelength ($\lambda/4$) criterion at the target operating frequency, enabling resonant amplification of particle displacement at the horn mouth. As a result, horn-loaded PZT transducers are usually narrowband devices operating at discrete frequencies, most commonly in the range of tens to hundreds of kilohertz. Despite their limited bandwidth and relatively large physical dimensions, these devices remain attractive for air-

 doi:10.20944/preprints202602.0014.v1

coupled applications requiring high acoustic output, long-range transmission, and mechanical robustness. Air-coupled horn-loaded PZT transducers typically employ a piezoelectric ceramic with a diameter in the range of 5-15 mm or 20-30 mm, and a thickness generally between 0.3 and 2 mm. The electrode materials used are commonly silver or nickel. The horn is usually fabricated in aluminium, steel or titanium and can feature a conical, exponential or stepped geometry. In quarter-wavelength designs, horn length is approximately equal to $\lambda/4$ at the operating frequency, while the overall horn length typically ranges from 10 to 100 mm. the backing material consists of dense, highly lossy metals or composite materials. These transducers usually operate at frequencies between 20 and 200 kHz and are designed for resonant, narrowband operation.

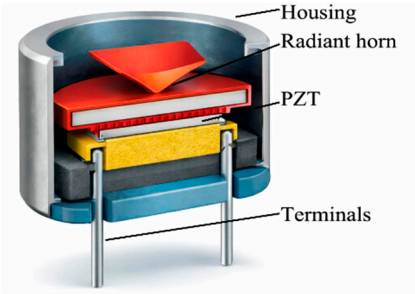

Figure 5. 3D representation of a horn-loaded piezoceramic ultrasonic transducer for air-coupled applications.

3.4. Piezopolymeric Sensor Design

Piezopolymer materials, particularly PVDF and its copolymers, have been extensively investigated as enabling technologies for ACU sensing due to their low acoustic impedance, mechanical flexibility, and broadband response [94]. Since the first demonstrations of curved and cylindrical PVDF film transducers in the 1970s, these materials have emerged as a viable alternative to conventional piezoceramic devices for ultrasonic operation in air, especially in the low-frequency range (20–100 kHz) (see Figure 6) [95].

Unlike piezoceramics, PVDF-based sensors primarily exploit extensional (d_{31}) vibration modes. When combined with tailored geometries—such as cylindrical, hemi-cylindrical, semi-conical, truncated-conical, spiral, and quasi-spherical structures—these modes enable efficient acoustic radiation in air while maintaining low quality factors and wide fractional bandwidths. The evolution of sensor design has therefore been largely geometry-driven, aiming to optimize bandwidth, sensitivity, directivity, and sound pressure level through control of bending radius, clamping conditions, and effective radiating aperture.

More recent developments have introduced non-uniform curvature and bio-inspired geometries, including spiral-shaped and quasi-spherical transducers [96]. These configurations support multiple resonance modes, enabling broadband operation and quasi-omnidirectional radiation patterns. Such features are particularly advantageous for ACU applications characterized by strong attenuation and low SNR, including biomedical monitoring, robotic perception, and biomimetic sonar [97,98].

From a system-level perspective, piezopolymer ultrasonic sensors are especially attractive as receivers, owing to their low permittivity and high open-circuit voltage sensitivity [99]. However, their lower electromechanical coupling compared to piezoceramics makes overall performance strongly dependent on the design of high-impedance, ultra-low-noise electronic interfaces [100]. Consequently, recent works increasingly adopt co-design strategies that jointly address transducer geometry, electronic front-end optimization, and advanced signal processing to overcome the intrinsic limitations of ultrasonic propagation in air.

 doi:10.20944/preprints202602.0014.v1

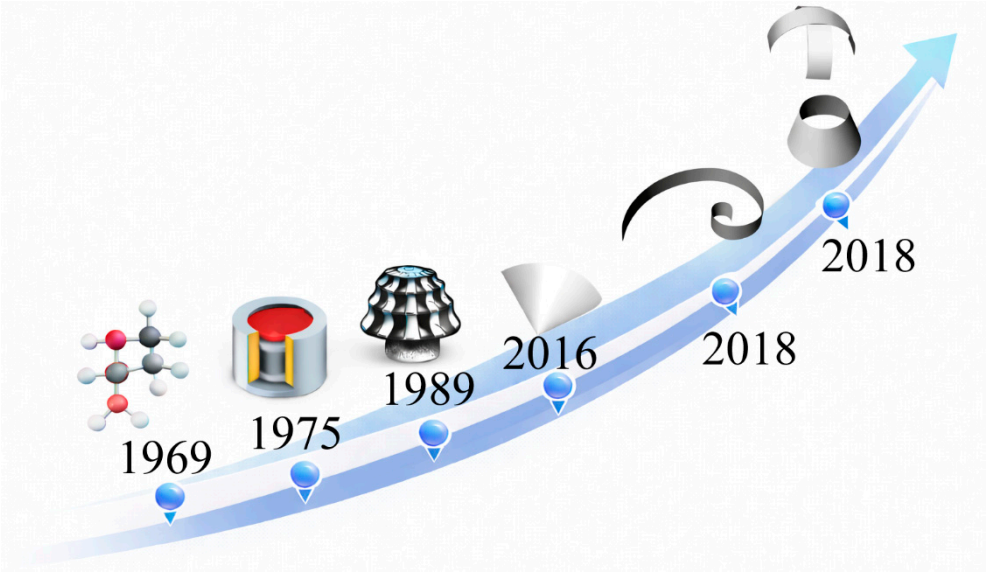

Figure 6. Evolution of PVDF ultrasonic transducer geometries for air-coupled applications along the timeline shown. In 1969, the discovery of PVDF piezoelectricity enabled lightweight piezopolymer ultrasound transducers. Early air-coupled implementations adopted cylindrical shells (1975), followed by hemi-cylindrical geometries (1989) to improve beam shaping and sensitivity. Semi-conical designs (2016) introduced additional control over directivity and spatial coverage. From 2018 onward, truncated-conical and spiral-shaped architectures were proposed to further tailor bandwidth and radiation patterns, culminating in quasi-spherical concepts aimed at widening angular coverage under air-propagation constraints.

Table 4. Summary of PVDF In-Air Ultrasonic Sensor Geometries

Geometry	Frequency (kHz)	Bandwidth (kHz)	Directivity	Sensitivity (dB)	Applications	Ref.
Cylindrical	40, 80	8, 10	H: 360 V: ±40	-76, -90	Positioning, ranging	[18]
Hemi-cylindrical	30–65	35	H: - V: ±15	-52	Obstacle detection	[18]
Semi-conical	24–36	12	H: ±50 V: ±60	N/A	Robotic sensing	[75]
Truncated conical	25–36	11	H: 360 V: ±70	N/A	3D positioning	[75]
Spiral-shaped	30–95	~60	H: 360 V: 360	H: -89.1 to -96.1 V: -94.2 to -103.8	Biomimetic sonar	[96]
Quasi-spherical	30–50	20	H: 360 V: ±120	N/A	Localization	[18]

PVDF in-air ultrasonic transducers have been explored both for contactless monitoring of small surface motions relevant to physiological sensing [18] and for pulse–echo ranging/localization within assistive and robotic perception frameworks inspired by biosonar [97,98]. Geometry-tailored architectures – such as truncated-conical and spiral transducers – further demonstrate how curvature can be engineered to satisfy application-driven requirements on beam pattern, coverage, and sensitivity [75,96]. Although several PVDF-based copolymers have been reported to exhibit enhanced piezoelectric properties compared to pristine PVDF, their large-scale availability and commercial adoption remain limited, which has so far constrained their widespread use in practical air-coupled ultrasonic transducer implementations.

 doi:10.20944/preprints202602.0014.v1

3.5. MEMS-Based Sensor Design

MEMS ultrasonic transducers have emerged as a complementary technology to piezopolymer-based sensors for ACU, particularly in applications requiring miniaturization, dense arrays, and electronic beamforming [101,102].

The two main architectures—capacitive micromachined ultrasonic transducers (CMUTs) and piezoelectric micromachined ultrasonic transducers (PMUTs)—differ in transduction principle, material stack, and achievable performance in air [103]. CMUTs typically rely on electrostatically actuated micromachined membranes and are often operated in off-resonance conditions to achieve wide fractional bandwidth. Representative air-coupled CMUT designs report membrane lateral dimensions on the order of 32 × 32 μm² with vacuum gaps around 250 nm, enabling broadband operation. As an example, an electrostatic air ultrasonic transducer with an active area of 3.3 × 3.3 mm² operating at 40 kHz achieved approximately 82 dB SPL (re 20 μPa) at 8.9 cm under a 24 V bias. PMUTs exploit thin-film piezoelectric stacks deposited on micromachined membranes and typically operate in flexural vibration modes. Compared to CMUTs, PMUTs generally require lower driving voltages and simpler electronic interfaces [71].

Air-coupled PMUTs based on single-crystal PZT have demonstrated sound pressure levels up to 100.3 dB SPL at 40 kHz measured at 33 cm, while ScAlN thin-film PMUT arrays have reported SPL values exceeding 120 dB at 10 cm, highlighting the benefits of array-based actuation at low ultrasonic frequencies [100]. By contrast, PVDF piezopolymer transducers exploit geometry-driven resonance using thin poled films operating primarily in d31 mode. Typical constructions reported in the literature include 40 μm PVDF films with ~200 nm aluminum electrodes for hemi-cylindrical devices, 28 μm films for semi-conical geometries, and 30 μm films with ~5 μm silver-ink electrodes for truncated-conical designs, with operational frequencies spanning approximately 20–100 kHz depending on curvature and boundary conditions.

Table 5. Summary of MEMS Ultrasonic Sensor Geometries

Technology	Geometry	Materials	Dimensions	Frequency range (kHz)	Bandwidth trend	SPL (examples)	Ref.
CMUT	membrane	Si/SiN	≈32 × 32 μm²; ≈250 nm gap	20-100		≈82 dB @ 40 kHz (8.9 cm)	[103]
PMUT	membrane	PZT or AlN/ScAlN	tens–hundreds μm	≈40		100.3 dB @ 40 kHz (33 cm); >120 dB @ 10 cm (array)	[104]

4. Electronic Interface for Low-Frequency Ultrasonic Sensors

Low-frequency ACU sensing represents one of the most challenging operational regimes for ultrasonic systems from an electronic interface perspective. Unlike contact-based ultrasonic techniques, where acoustic coupling media such as water or gels enable relatively efficient energy transfer, ACU systems must operate across a severe acoustic impedance mismatch between air and solid media. This mismatch results in extremely high transmission losses, which may easily exceed 80–100 dB depending on frequency, propagation distance, and target properties [105]. Consequently, the amplitude of the acoustic wave reaching the receiving transducer is reduced, and only a small fraction of the transmitted energy is converted back into an electrical signal.

From an electronic perspective, this attenuation fundamentally changes the role of the receive chain. Since the electrical signal generated at the transducer terminals is often close to the intrinsic noise floor of conventional analog front-end circuits, signal extraction is highly dependent on the electronic interface characteristics. Accordingly, the front-end cannot be regarded as a signal-conditioning stage of secondary importance; instead, they become a primary performance-limiting

 doi:10.20944/preprints202602.0014.v1

element of the entire sensing system. Furthermore, marginal improvements in front-end noise performance or impedance matching can provide significant gains at the system level, in some cases comparable to those obtained through direct transducer optimization.

These challenges are further compounded by the electrical characteristics of transducers commonly employed in low-frequency ACU applications. Piezoelectric polymer sensors, such as PVDF, are widely used because of their broadband response, mechanical flexibility, and more favorable acoustic impedance relative to air. However, from an electrical point of view, these devices typically exhibit high output impedance and predominantly capacitive behavior. When interfaced with non-ideal electronics, this combination can lead to unpleasant drawbacks as signal loading, bandwidth reduction, and increased susceptibility to parasitic capacitances associated with cables, packaging, and input devices. It is therefore essential an accurate circuital-level equivalent model of the sensor. This is especially complex since it not only depends on the material used, but also on the actual shape of the transducer, as shown in Figure 7 where an equivalent circuit is shown for a PVDF-based hemi-cylindrical (Figure 7a) and spiral (Figure 7b) shapes.

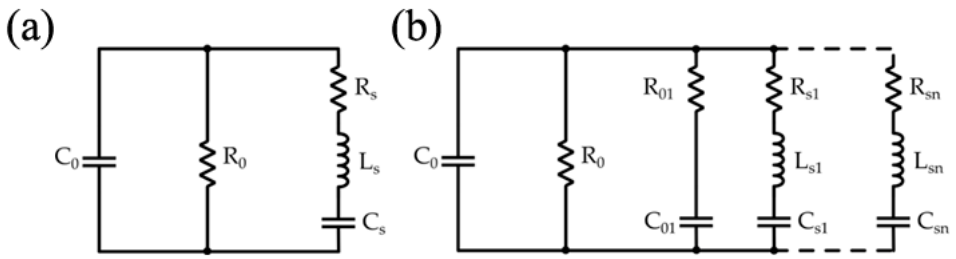

Figure 7. (a) Butterworth-Van Dyke model for Hemi-cylindrical PVDF transducer. (b) Butterworth-Van Dyke model for Spiral-Shaped PVDF transducer.

Noise considerations are particularly critical in low-frequency ACU systems as well. In many practical scenarios, electronic noise dominates over acoustic noise sources, especially at low frequencies where environmental and mechanical disturbances may also contribute. Analytical and experimental studies indicate that the total noise floor results from a complex interaction between the thermal noise associated with the real part of the transducer impedance, the voltage and current noise of the active devices, and additional contributions introduced by biasing networks and feedback components [105].

Nevertheless, generic receiving chain for ultrasonic sensing comprises the front-end preamplifier, typically a very low-noise, relatively low-gain stage, intermediate analog conditioning stages, and the digitization and post-processing blocks (see Figure 1b in Section 2.1).

While this architecture is common to most ultrasonic systems, its implementation in low-frequency ACU applications is subject to significantly tighter constraints. In particular, the first stage plays the most important role, as it directly interfaces with the transducer and largely determines the effective sensitivity, bandwidth, and noise performance of the entire system. The primary role of the front-end preamplifier is to convert the weak electrical signal generated by the ultrasonic transducer into a form suitable for further processing, while preserving as much signal integrity as possible. In ACU systems, this task is complicated by the combination of very low signal amplitudes and high source impedance. Consequently, the preamplifier must provide sufficient gain without excessively loading the transducer, while simultaneously maintaining a low input-referred noise across the frequency band of interest.

Recent reviews on ultrasonic preamplifier design emphasize that the optimal receive chain architecture is highly dependent on the electrical nature of the transducer and the target application [106]. The choice of topology often depends on the transducer type; for instance, voltage amplifiers (VA) are typically preferred for piezoelectric sensors like PMUTs, while charge-sensitive amplifiers (CSA) or transimpedance amplifiers (TIA) are better suited for CMUT that generate currents [105].

 doi:10.20944/preprints202602.0014.v1

Voltage-mode front ends rely on high input impedance amplifiers to sense the voltage generated by the piezoelectric transducer while minimizing signal loading. In principle, this approach is well suited for piezoelectric devices, which can be modeled as voltage sources in series with a capacitive kind impedance. In practice, however, the extremely weak signals encountered in ACU systems require high gain already at the first amplification stage. Owing to the finite gain–bandwidth of operational amplifiers, increasing the closed-loop gain directly reduces the available bandwidth, thereby limiting the ability to process broadband ultrasonic signals. Figure 8a shows a basic example circuit for the voltage mode approach: a voltage buffer that ensures an extremely high input impedance while maintaining very low noise characteristic, thanks to its unitary gain.

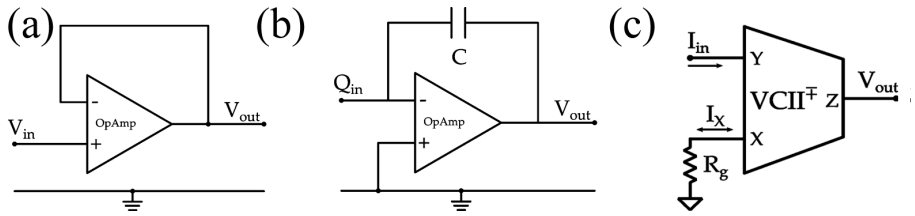

Figure 8. (a) Voltage buffer configuration ensuring high input impedance and low noise characteristics. (b) Op-Amp-based charge amplifier configuration. (c)VCII-based transimpedance configuration

Charge-sensitive amplifiers have been widely proposed as an alternative to mitigate these limitations. By integrating of the charge generated by the transducer onto a feedback capacitor, CSAs offer reduced sensitivity to input capacitance variations and improved robustness against cable and parasitic capacitances. Comparative studies have shown that, under the presence of large parasitic capacitances, charge amplifiers can outperform simple voltage amplifiers in terms of stability and noise behavior [107]. Despite these advantages, charge-based architectures do not eliminate the fundamental limitations imposed by voltage-mode operation. The achievable bandwidth of a CSA remains constrained by the open-loop characteristics of the operational amplifier, and the feedback network introduces additional noise sources that may become dominant at low frequencies. Figure 8b shows a basic example circuit for the “charge mode” approach, where charge is evaluated via an Op-Amp-based charge amplifier.

The discussed limitations of conventional voltage-mode and charge-based front-end architectures have motivated an increasing interest in alternative interface architectures. Among these, current-mode and mixed-mode read-out systems have emerged as particularly attractive solutions for ultrasonic sensing, especially under the extreme operating conditions imposed by low-frequency air-coupled applications. Current-mode front ends differ from traditional voltage-mode approach because the signal generated by the transducer is processed primarily in the current domain rather than being immediately converted into a voltage through high-impedance amplification. This shift offers several intrinsic advantages. First, current-mode architectures are not constrained by gain–bandwidth product limitations, as signal amplification is not strictly tied to high loop gain and global feedback. As a result, wideband operation can be achieved without sacrificing gain, a property that is particularly beneficial in broadband ACU systems where both sensitivity and temporal resolution are critical. From a noise point of view, current-mode processing can interact with high-impedance and capacitive transducers. By presenting a low-impedance input node to the sensor, current-mode interfaces can reduce the influence of parasitic capacitances and leakage paths that typically degrade the performance of voltage-mode front ends. At the same time, the transformation of the sensor signal into a current allows noise contributions to be shaped differently across the frequency band, potentially improving the overall SNR if properly designed.

Among current-mode building blocks, second generation current conveyors (CCII) and their derivatives have attracted considerable attention in sensor interface applications [108–110]. In particular, the second-generation voltage conveyor (VCII) has been proposed as a mixed-mode solution that combines current-domain input processing with a low-impedance voltage output. As

 doi:10.20944/preprints202602.0014.v1

the dual counterpart of the well-known CCII, the VCII enables current-mode sensing while directly providing a voltage output compatible with conventional analog and mixed-signal processing stages. Recent studies on VCII-based signal conditioning have highlighted their architectural simplicity, gain programmability, and suitability for low-voltage and low-power operation [111]. Figure 8c shows a VCII-based transimpedance configuration.

Overall, the comparative analysis between current-mode and voltage-mode highlights that conventional voltage-mode and charge-sensitive front ends remain satisfactory reference solutions but operate near their practical limits in low-frequency air-coupled ultrasonic applications. Current-mode and mixed-mode architectures, although more demanding from a design point of view, provide a more flexible and scalable framework for addressing the extreme attenuation, noise dominance, and bandwidth requirements characteristic of ACU systems. These considerations motivate continued research on interface architectures that explicitly leverage current-domain processing and electronics sensor co-design to improve the performance of ACU sensing.

A comparative overview of several state-of-the-art amplifiers and analog interface circuits developed for ACU signal acquisition is presented in Table 6, highlighting the main performance trends emerging from recent literature and emphasizing the differences between voltage-mode and current-mode implementations.

Table 6. Summary of state-of-the-art electronic interfaces for low-frequency ultrasonic sensors.

Transducer	Front-end	Frequency Range	Noise or Sensitivity focus	Key Advantages	Ref.
Air-coupled piezoelectric	Voltage-mode low-noise preamplifier	400 – 800 kHz	Analytical SNR optimization	Rigorous noise modelling including transducer	[105]
AlN PMUT array	Voltage vs charge amplifier (CMOS)	~3 MHz (liquid)	VA shows superior SNR; input noise of 0.08 pA/√Hz (VA) vs 0.15 pA/√Hz (CSA)	CMOS integration, Low power, removal of crowbar current, and reduced parasitic elements	[107]
PVDF hydrophone	Integrated voltage preamplifier	100 kHz – 1.5 MHz	High sensitivity PVDF receiver (1.62 V/MPa)	MRI compatibility and low cost	[112]
Logarithmic spiral-shaped PVDF	VCII-based TIA	20 – 80 kHz	Sensitivity ≈ −100 dB	Low power consumption (6 mA), simple single-stage architecture, bypasses GBW constraints	[113]
PVDF spiral ACU	VCII-based TIA + filter	20 – 100 kHz	Sensitivity comparable to commercial sensors (-120 to -92 dB)	Bio-inspired design (mammalian cochlea), 360° omnidirectional pattern, easy fabrication	[114]
Miniature PVDF (110 μm)	Unity gain preamplifier (LMH6639 Op-Amp)	0.51 MHz – 5.4 MHz	High sensitivity (2.36–3.87 V/MPa); noise floor of 0.21 kPa at 1.1 MHz	Extremely low cost (< 4 USD), wide acceptance angle (54° at 1.1 MHz), and subharmonic detection	[115]

5. Signal Processing Strategies

In ACU systems, signal processing is an integral of the measurement architecture rather than a simple post-processing phase. The high attenuation of ultrasound in air, wavefront dispersion and strong dependence on environmental conditions make the useful signal intrinsically weak and susceptible to distortion, especially in non-invasive biomedical applications. Accordingly, the literature converges on the view that overall performance of ACU systems critically depends on the

 doi:10.20944/preprints202602.0014.v1

synergy among sensor design, electronic architecture, and adopted signal processing strategies [116–118].

While this system-level perspective is widely acknowledged, the biomedical ACU literature still lacks a structured comparison of post-processing strategies in relation to operating frequency, dominant noise sources, and achievable signal quality. Most contributions address signal processing as an application-specific design choice rather than as a dimension to be analysed comparatively across studies. Consequently, the impact of different processing approaches on robustness, sensitivity, and system complexity is often implicit and difficult to generalise.

A first distinction emerges when considering the temporal and spatial scale of the physiological phenomena under investigation. Respiratory activity and posture-related movements, which involve slow, large-amplitude movements, TOF estimation and envelope tracking remain the most widely used approaches [44–46]. Their prevalence is mainly due to their inherent robustness to amplitude fluctuations, moderate tolerance to environmental variability, and low computational burden. However, the achievable displacement resolution is fundamentally constrained by the ultrasonic wavelength and by the accuracy of TOF estimation under low SNR conditions, which limits their suitability for fine motion analysis. In contrast, heart-induced chest wall vibrations and subtle biomechanical activities, which target micro-movements, are mainly based on phase demodulation and Doppler-based processing [40–43,47]. By exploiting phase or instantaneous frequency variations of the received ultrasonic waveform, these techniques enable sub-millimetric sensitivity that cannot be achieved through TOF-based methods. Several studies report reliable heart-rate extraction in fully non-contact configurations, even though light clothing. Nonetheless, this increased sensitivity is accompanied by heightened vulnerability to macroscopic body motion, oscillator phase noise, and thermal drift, thereby imposing stricter constraints on electronic stability, synchronization, and calibration.

To mitigate the severe attenuation and noise inherent to ultrasonic propagation in air, many works adopt coded excitation and correlation-based post-processing schemes. Frequency-modulated chirp signals and coded pulse signals, combined with adaptive filtering methods or pulse compression algorithms, make it possible to increase the transmitted power without violating the constraints of acoustic safety [120,121]. These methods have demonstrated a significant improvement in the resistance to detection in a low signal-to-noise ratio, particularly at high frequencies. However, their effectiveness may be compromised by multipath propagation and correlation ambiguities, which necessitate additional signal conditioning or spatial filtering stages.

Spatial processing provides an additional information for post-processing optimisation in biomedical ACU systems. Multi-channel averaging and digital beamforming techniques are increasingly employed to enhance directivity, suppress clutter, and stabilise signal quality in the presence of environmental disturbances [41,65]. In array-based configurations, beamforming has been shown to improve the continuity and reliability of respiratory and cardiac estimates, especially in uncontrolled or home-monitoring scenarios. These benefits, however, come with the cost of higher complexity, power, and computation, which could make them unsuitable for wearable or chronic monitoring applications.

A comparative analysis of post-processing approaches reported in the biomedical ACU literature is provided in Table 7. The table highlights the range of operating frequencies, noise types, and types of signal quality improvement provided by post-processing. The key takeaway is that there is not one method that performs best under all circumstances. Instead, a good signal extraction procedure involves a trade-off between micro-motion sensitivity, resistance to environmental/motion noise, and overall system complexity.

Table 7. Post-processing strategies for ACU in biomedical applications.

Application domain	Post-processing technique	Typical frequency range	Dominant noise source	Signal quality improvement	Ref.

 doi:10.20944/preprints202602.0014.v1

Respiration monitoring	TOF / envelope tracking	20–40 kHz	Environmental noise, drift	Robust distance estimation	[41,45,46]
Cardiac monitoring	Phase / Doppler analysis	~40 kHz	Motion artefacts, phase noise	Sub-mm displacement sensitivity	[40–42,46]
Vital signs (HR + RR)	Hybrid (TOF + phase/Doppler)	~40 kHz	Mixed: macroscopic body motion, drift, phase noise, multipath	Simultaneous HR/RR extraction; improved stability vs single domain (TOF for large motion, phase for micro-motion)	[48,49]
Low-SNR sensing	Chirp + matched filtering	30–90 kHz	Mixed (motion + electronic)	Improved stability vs single domain	[119,120]
Multi-target sensing	Beamforming / array processing	40–80 kHz	Attenuation, broadband noise	Spatial filtering and robustness	[41,65]
Feature extraction	ML-assisted post-processing	Application-dependent	Non-stationary noise	Improved estimation robustness	[121–123]

The use of machine-learning-based approaches introduces non-negligible criticalities, especially in terms of model generalisation across different subjects, environmental conditions and hardware configurations. Moreover, the limited interpretability of many data-driven solutions is a critical aspect in the clinical field, where transparency of the decision-making process is often a prerequisite. The trade-off between signal sensitivity, environmental robustness, and implementation complexity is further summarised in Table 8. TOF-Based and Simple Filtering Techniques are on the low-complexity end of the spectrum and are appropriate for embedded designs. Phase- and Doppler-based methods offer the best sensitivity values but require tight control of system stability. Correlation- and multi-channel techniques are more robust but require more hardware resources and computation load.

Table 8. Trade-off between sensitivity, robustness, and complexity in ACU signal processing.

Processing strategy	Sensitivity to micro-movements	Environmental robustness	Hardware complexity	Computational complexity
Basic filtering	Low-Medium	Medium	Low	Low
TOF tracking	Medium	High	Low	Low
Chirp/correlation	High	Low	Medium	Medium-High
Beamforming/arrays	High	High	High	Very high
Hybrid DSP + AI	Very high	Variable	High	Very high

Finally, post-processing choices are intrinsically linked to the ultrasonic carrier frequency, since attenuation, bandwidth, and achievable displacement resolution in air are strongly frequency dependent. As summarised in Table 9, lower frequencies favour robustness and operating range, whereas higher frequencies enable finer spatial resolution at the cost of increased attenuation and noise susceptibility [31,35].

 doi:10.20944/preprints202602.0014.v1

Table 9. Relationship between ultrasonic frequency range and signal quality in air-coupled biomedical ultrasound.

Frequency range	Typical applications	Preferred post-processing	Main limitations
20-30 kHz	Respiration, gross motion	TOF, envelope	Limited spatial resolution
~40 kHz	Vital signs, cardiac monitoring	Phase/Doppler, hybrid	Sensitivity to motion artefacts
60–100 kHz	Fine motion, arrays	Chirp, beamforming	Strong air attenuation

Overall, this comparative analysis indicates that signal processing in biomedical ACU systems should be conceived as part of an integrated system-level co-design framework. Post-processing operation can partially compensate for the physical limitations imposed by air propagation, but they cannot fully overcome them. Therefore, optimal performance requires proper integration of frequency selection, sensor and electronic interface design, and processing complexity according to the specific biomedical objective.

The first level of processing, dedicated to signal pre-processing, aims to increase the signal-to-noise ratio and stabilise the information acquired before the subsequent analysis stages [124]. A typical pre-processing chain, widely adopted in non-contact biomedical applications, and includes bandpass filtering centred on the operating frequency of the transducer, amplitude normalisation, and separation of the physiological components of interest. Studies on airborne ultrasonic sensors based on polymeric materials and bio-inspired architectures show how such strategies can significantly reduce environmental interference without compromising the dynamic response of the system [116,125].

In non-contact physiological monitoring applications, such as respiratory activity assessment, low-pass filters are also used to isolate slow signal components, while offset removal and normalisation operations are essential to compensate for slow drifts due to electronic instability or environmental variations [126,127]. However, overly selective filtering can result in a loss of temporal information, limiting the system ability to detect rapid changes or physiologically relevant transitions [128]. Time of flight (TOF) strategies are one of the most established approaches in ACU systems. TOF estimation enables the calculation of distance variations between the sensor and the target that are directly related to respiratory motion or slow body movements.

TOF methods have been found to be robust to amplitude noise and provide a high level of physical interpretability, thus making them suitable for long-term monitoring in uncontrolled environments [129]. Additionally, differential TOF analysis helps to compensate for changes in the speed of sound in ambient air due to variations in temperature and humidity, which is very important in biomedical applications [126,127]. However, there remains an intrinsic limitation related to reduced sensitivity to micro-movements, which limits its use to respiratory monitoring rather than cardiac activity detection. To overcome these limitations, numerous studies propose the analysis of the phase of the ultrasonic signal or the use of Doppler techniques, capable of detecting sub-millimetre micro-movements with high sensitivity. Compared to TOF techniques, phase analysis offers significantly higher spatial resolution, making it possible to detect cardiac activity even in completely non-contact configurations [117,118]. However, these systems involve increased complexity in electronic systems and are highly sensitive to macroscopic motions of the body.

The need for coherent demodulation and the presence of oscillators impose a major constraint in terms of system calibration. At the same time, strategies based on the use of modulated signals and correlation techniques have been explored to improve the signal-to-noise ratio in conditions of strong attenuation. The use of coded pulses or chirp signals allows the transmitted energy to be increased while keeping the peak acoustic pressure limited, a particularly important requirement in the biomedical field. Studies on airborne ultrasonic systems show that these approaches are more robust than simple pulses, especially in complex indoor environments [129]. However, the presence of

 doi:10.20944/preprints202602.0014.v1

multipath phenomena can generate ambiguity in the correlation function, requiring additional processing stages and increasing the overall computational load. A further evolution of signal processing strategies in ACU systems is represented by multi-channel processing and digital beamforming.

The conceptual diagram of an airborne ultrasonic array with digital beamforming for non-invasive biomedical applications demonstrates how spatial processing improves the directivity of the system, reducing the impact of unwanted reflections and increasing the stability of physiological estimates, while supporting multi-target applications [116,118]. However, these advantages are accompanied by a significant increase in hardware complexity and power consumption, limiting their use in wearable devices or long-term home monitoring systems. In recent years, ACU signal processing strategies have been further improved through integration with data-driven approaches and artificial intelligence systems. In this context, traditional signal processing is often used to extract physically interpretable features, which are then processed using machine learning models to improve the accuracy and robustness of the system [130,131]. Despite the high potential, the literature highlights critical issues related to model generalisation, dependence on training data, and limited interpretability of decisions, aspects of particular relevance in the clinical setting.

A comparative summary of the main signal processing strategies adopted in ACU systems is shown in Table 10, which shows that there is no universally optimal solution, but rather a compromise between sensitivity to micro-movements, environmental robustness, and computational complexity, which must be evaluated according to the specific application. The comparative analysis shown in Table 10 clearly highlights how the selection of signal processing strategies in ACU systems should be guided primarily by the trade-off between sensitivity to micro-movements, environmental robustness and computational complexity, rather than by the search for a universally optimal solution.

Table 10. Comparison between the main signal processing strategies in ACU systems.

Strategy	Sensitivity to micro-movements	Environmental robustness	Complexity	Ref.
Filtering and pre-processing	Low–Medium	Medium	Low	[126,127]
TOF	Medium	High	Low	[126,127,129]
Phase/Doppler analysis	High	Low	Medium – High	[117,118]
Correlation and modulated signals	Medium–High	Medium	High	[129]
Multi-channel beamforming	High	High	Very high	[118]
Hybrid approaches with AI	Very high	Variable	Very high	[130,131]

Filtering and pre-processing techniques, while representing the minimum necessary level in any ACU architecture, are inherently limited in terms of sensitivity and cannot, on their own, support applications that require the detection of complex physiological micro-movements. In contrast, TOF-based approaches show a favourable combination of environmental robustness and simplicity of implementation, making them particularly suitable for long-term respiratory monitoring in uncontrolled environments, but less effective for cardiac applications. Strategies based on phase analysis and Doppler techniques emerge as the most suitable for detecting sub-millimetre micro-movements, as confirmed by the work reported in [117,118]. On one side, a high sensitivity is balanced by a larger vulnerability with respect to macroscopic motions and a requirement for system stability and calibration. On the other side, a use of modulated signals and correlation processing

 doi:10.20944/preprints202602.0014.v1

provides a larger robustness with respect to noise and attenuations but also provides ambiguities with respect to multipaths and a complexity increase that need to be balanced with hardware capabilities.

Multi-channel beamforming solutions are the most comprehensive solution from a performance perspective. They provide very good sensitivity with robustness to environmental changes. Nevertheless, as seen from Table 7, this solution incurs maximal complexity with respect to hardware and energy. Thus, this solution is best suited for fixed installations rather than wearable systems and home monitoring. Finally, hybrid approaches that integrate traditional signal processing and artificial intelligence models are a promising direction for overcoming the limitations of individual techniques. The possibility of combining physically interpretable features with data-driven models allows for improved system sensitivity and robustness, as shown in [130,131]. However, the adoption of such approaches in the clinical setting requires careful evaluation of model generalisability, decision transparency, and computational sustainability, aspects that still represent an open challenge in the design of reliable and clinically validatable ACU systems. In this context, recent studies increasingly highlight the role of artificial intelligence not only as a final classification or regression tool, but as an advanced post-processing stage for airborne ultrasonic signals. In such approaches, pre-processed ACU signals are fed into machine learning algorithms. These signals can be converted into time-frequency domain signals so that the machine learning algorithms can address issues like nonlinear attenuation, multipath, and environment introduced when ultrasound signals travel through air. These data-driven post-processing techniques enable the extraction of robust physiological patterns even under low signal-to-noise ratio conditions. Although several methodological advances have initially been developed in the broader field of non-contact sensing, including microwave-based vital sign monitoring, the underlying signal processing and learning paradigms are directly transferable to ACU systems. Recent review studies demonstrate that machine learning-based post-processing significantly improves the stability and accuracy of vital sign estimation in dynamic and uncontrolled conditions, compared to purely deterministic signal processing pipelines [130]. This is particularly important in the case of ACU systems implemented in practical biomedical applications, where variability is difficult to control.

A further trend that is currently emerging is the incorporation of artificial intelligence directly after ultrasonic signal processing pipelines. Advances in intelligent nano- and micro-scale sensors and actuators indicate that the combination of physically interpretable ultrasonic features with embedded learning models can support local decision-making and edge-level processing, thereby reducing latency and dependence on external computational resources [131]. In this framework, conventional signal processing retains a fundamental role in ensuring physical interpretability, while artificial intelligence provides higher-level robustness and adaptability.

Nevertheless, the literature consistently notes that AI-based post-processing of air-coupled ultrasonic signals still faces significant challenges. Key issues include the availability of representative training datasets, the generalisation capability of learned models across different subjects and environmental conditions, and the limited interpretability of model outputs. These problems become even more relevant in a clinical setting where transparency, accuracy, and validation are crucial. Future research will focus in the developing of hybrid solutions balancing accuracy and understandability.

6. Discussion and Conclusions

This review highlighted how low-frequency ACU is consolidating as a fully non-contact sensing modality in two converging biomedical domains: (i) contactless monitoring of physiological micro-movements (respiration and cardio-mechanical activity) and (ii) medical/assistive robotics and human-machine interfaces requiring short-range ranging, tracking, and coarse geometric reconstruction. Across these domains, the primary performance bottleneck is not the sensing principle itself, but the system-level co-design needed to reliably extract weak echoes in air under realistic environmental and motion variability [17,18,21]. From a physics perspective, the pronounced

 doi:10.20944/preprints202602.0014.v1

acoustic-impedance mismatch at the transducer-air interface, together with the frequency-dependent air attenuation, imposes an intrinsic trade-off among operating range, spatial resolution, and robustness [32,33]. In the 20-100 kHz band, practical systems typically favor lower-frequency operation to extend range and mitigate attenuation, while relying on waveform engineering (bursts, chirps, coded sequences) and coherent processing (phase/Doppler) to regain sensitivity to sub-millimetric motion [40–44,119,120]. Temperature and humidity dependence, multipath propagation, and clutter further motivate calibration and compensation strategies and, where feasible, spatial filtering via multichannel or array-based acquisition [41,65]. Sensor technologies are consequently evolving along two complementary directions. Horn-loaded or matched PZT transducers remain attractive for high-SPL transmission and longer-range operation, but their narrowband response and bulk can limit wearable/embedded integration. Piezopolymer solutions (PVDF and related ferroelectric/ferroelectret architectures) offer broadband operation and more favorable acoustic impedance and have proven particularly effective as receivers when paired with ultra-high input impedance, low-noise interfaces [18,24,105]. MEMS-based CMUT/PMUT arrays, in turn, enable dense multi-channel architectures and electronic beamforming to stabilize performance in cluttered scenes, albeit often at the cost of increased system complexity and stringent drive and interface requirements [22,103,104]. Concerning electronic interfaces, receive chain—especially the first preamplifier stage— constitutes the main system bottleneck (not a secondary "conditioning" block): small improvements in input noise or impedance matching can yield system-level gains comparable to transducer optimization. Since voltage/charge approaches operate near practical limits in low-frequency ACU, current-mode and mixed-mode interfaces (e.g., CCII/VCII-based transimpedance) are increasingly attractive: they can avoid GBW constraints, better tolerate parasitic components via low-impedance input nodes, and reshape noise for improved SNR—at the cost of more demanding design. Along the paper we have highlighted competitive sensitivity and simple, low-power VCII/TIA solutions in the 20–100 kHz range alongside established voltage/charge implementations at higher frequencies. On the algorithmic side, TOF/envelope tracking generally provides robust respiration monitoring, whereas phase/Doppler processing is required for cardiac micro-motion but demands higher stability and motion-artifact handling. Hybrid pipelines and adaptive filtering can help bridge these operating regimes [40–49]. Despite rapid progress, the surveyed literature remains heterogeneous in reporting practices, which hinders reproducibility and cross-study comparison. To support biomedical translation, a minimum reporting set should consistently include: the operating frequency band and excitation waveform; emitted SPL and reference distance; receiver sensitivity and calibration procedure; directivity/beamwidth; complete front-end schematic or equivalent parameters (input impedance, gain, bandwidth, input-referred noise); digitization settings; environmental conditions (temperature/humidity) and compensation; and evaluation protocols/metrics (e.g., RR/HR error under controlled motion and through-clothing conditions) [18,29,40–46]. Establishing shared benchmarking datasets and test scenarios would further accelerate objective comparison of sensors, interfaces, and processing strategies. Looking forward, the most impactful advances are expected to come from co-design approaches that jointly optimize transducer geometry/materials, low-noise interfaces, and application-aware processing. Emerging directions include flexible and large-area airborne arrays, multimodal fusion with optical/radar/inertial sensing to improve robustness, and interpretable AI-assisted post-processing for operation in low-SNR, multipath-rich environments [15,84,85,121–123,130,131]. Overall, low-frequency ACU is well positioned to enable privacy-preserving, contactless biomedical monitoring and assistive technologies; achieving clinical-grade reliability will require standardized validation workflows and system-level design rules that are portable across devices and deployment settings.

Author Contributions: Conceptualization, F.L., G.F. and S.A.P.; methodology, F.L., R.O. and E.S.; investigation, F.L., R.O. and E.S.; data curation; F.L., R.O. and E.S.; formal analysis; F.L., R.O., E.S. G.B. G.F. and S.A.P.; writing—original draft preparation, F.L., R.O., G.B. and E.S.; writing—review and editing, F.L., R.O., E.S., G.B.,

 doi:10.20944/preprints202602.0014.v1

G.F. and S.A.P.; visualization, G.B., G.F. and S.A.P.; supervision, G.F. and S.A.P. All authors have read and agreed to the published version of the manuscript.

Funding: This research received no external funding.

Data Availability Statement: No new data were created or analyzed in this study. Data sharing is not applicable to this article.

Conflicts of Interest: The authors declare no conflicts of interest.

References

1. Hassanpour, A.; Yang, B. Contactless Vital Sign Monitoring: A Review Towards Multi-Modal Multi-Task Approaches. *Sensors* **2025**, *25*, 4792.
2. Al-Naji, A.; Al-Askery, A.J.; Gharghan, S.K.; Chahl, J. A System for Monitoring Breathing Activity Using an Ultrasonic Radar Detection with Low Power Consumption. *J. Sens. Actuator Netw.* **2019**, *8*, 32.
3. Kabiri, M.; Cimarelli, C.; Bavle, H.; Sanchez-Lopez, J.L.; Voos, H. A Review of Radio Frequency Based Localisation for Aerial and Ground Robots with 5G Future Perspectives. *Sensors* **2022**, *23*, 188.
4. Tsao, J.Y.; Crawford, M.H.; Coltrin, M.E.; Fischer, A.J.; Koleske, D.D.; Subramania, G.S.; Wang, G.T.; Wierer, J.J.; Karlicek Jr, R.F. Toward smart and ultra-efficient solid-state lighting. *Advanced Optical Materials* **2014**, *2*(9), 809–836.
5. Madore, B.; Preiswerk, F.; Bredfeldt, J.S.; Zong, S.; Cheng, C.-C. Ultrasound-based sensors to monitor physiological motion. *Med. Phys.* **2021**, *48*, 3614–3622.
6. Niérat, M.-C.; Laveneziana, P.; Dubé, B.-P.; Shirkovskiy, P.; Ing, R.-K.; Similowski, T. Physiological Validation of an Airborne Ultrasound Based Surface Motion Camera for a Contactless Characterization of Breathing Pattern in Humans. *Front. Physiol.* **2019**, *10*, 680.
7. Abreu, D.; Toledo, J.; Codina, B.; Suárez, A. Low-Cost Ultrasonic Range Improvements for an Assistive Device. *Sensors* **2021**, *21*, 4250.
8. Qiu, Z.; Lu, Y.; Qiu, Z. Review of Ultrasonic Ranging Methods and Their Current Challenges. *Micromachines* **2022**, *13*, 520.
9. Diebold, C.A.; Salles, A.; Moss, C.F. Adaptive Echolocation and Flight Behaviors in Bats Can Inspire Technology Innovations for Sonar Tracking and Interception. *Sensors* **2020**, *20*, 2958.
10. Marzo, A.; Corkett, T.; Drinkwater, B.W. Ultraino: An Open Phased-Array System for Narrowband Airborne Ultrasound Transmission. *IEEE Transactions on Ultrasonics, Ferroelectrics, And Frequency Control* **2018**, *65*, 102–111.
11. Wu, Q.; Chen, Q.; Lian, G.; Wang, X.; Song, X.; Zhang, X. Investigation of an air-coupled transducer with a closed-cell material matching strategy and an optimization design considering the electrical input impedance. *Ultrasonics* **2021**, *115*, 106477.
12. Fiorillo, A.S. Noise analysis in air-coupled PVDF ultrasonic sensors. *IEEE Transactions on Ultrasonics, Ferroelectrics, And Frequency Control* **2000**, *47(6)*, 1432–1437.
13. Kelly, S.P.; Hayward, G.; Gomez, T.E. An air-coupled ultrasonic matching layer employing half wavelength cavity resonance, *2001 IEEE Ultrasonics Symposium. Proceedings. An International Symposium (Cat. No.01CH37263)*, Atlanta, GA, USA, **2001**, *2*, 965–968.
14. Xu, J.; Ye, Y.; Dong, T.; Yang, Z.; Pires, N.M.M.; Zhou, Y.; Tao, F.; Wang, J.; Zhang, J.; Luo, G.; Zhao, L.; Mao, Q.; Wang, Y.; Jiang, Z. State of the Art of Low-Frequency Acoustic Modulation: Intensity Enhancement and Directional Control. *Adv. Sci.* **2025**, *12*, 2410695.
15. Wang, S.; Mei, L.; Liu, R.; Jiang, W.; Yin, Z.; Deng, X.; He, T. Multi-modal fusion sensing: A comprehensive review of millimeter-wave radar and its integration with other modalities. *IEEE Communications Surveys & Tutorials* **2024**, *27*(1), 322–352.
16. Redij, R.; Kaur, A.; Muddaloor, P.; Sethi, A.K.; Aedma, K.; Rajagopal, A.; Gopalakrishnan, K.; Yadav, A.; Damani, D.N.; Chedid, V.G.; Wang, X.J.; Aakre, C.A.; Ryu, A.J.; Arunachalam, S.; Practicing Digital Gastroenterology through Phonoenterography Leveraging Artificial Intelligence: Future Perspectives Using Microwave Systems. *Sensors* **2023**, *23*, 2302.

 doi:10.20944/preprints202602.0014.v1

17. Chimenti, D.E. Review of air-coupled ultrasonic materials characterization. *Ultrasonics* **2014**, *54(7)*, 1804–1816.
18. Pullano, S.A.; Critello, C.D.; Bianco, M.G.; Menniti, M.; Fiorillo, A.S. PVDF ultrasonic sensors for in-air applications: a review. *IEEE Transactions on Ultrasonics, Ferroelectrics, And Frequency Control* **2021**, *68(7)*, 2324–2335.
19. Zhang, Y.; Jin, T.; Deng, Y. A low-voltage-driven MEMS ultrasonic phased-array transducer for fast 3D volumetric imaging. *Microsyst Nanoeng* **2024,** *10*, 128.
20. Peng, X.; Hu, L.; Liu, W.; Fu, X. Model-Based Analysis and Regulating Approach of Air-Coupled Transducers with Spurious Resonance. *Sensors* **2020**, *20*, 6184.
21. Rathod, V.T. A Review of Acoustic Impedance Matching Techniques for Piezoelectric Sensors and Transducers. *Sensors* **2020**, *20*, 4051.
22. Lin, J.L.; Kao, C.L.; Wu, S.W.; Hsu, H.J.; Lin, H.C.; Li, C.Y.; Chen, C.Y.; Huang, C.H. Air-coupled piezoelectric micromachined ultrasonic transducer array based on low-cost and large remnant polarization PZT thin film. *Sci Rep* **2025**, *15(1)*, 38158.
23. Demi, L. Practical Guide to Ultrasound Beam Forming: Beam Pattern and Image Reconstruction Analysis. *Appl. Sci*. **2018**, *8*, 1544.
24. Xin, Y.; Sun, H.; Tian, H.; Guo, C.; Li, X.; Wang, S.; Wang, C. The use of polyvinylidene fluoride (PVDF) films as sensors for vibration measurement: A brief review. *Ferroelectrics* **2016**, *502*(1), 28–42.
25. Van Neer, P.L.M.J.; Peters, L.C.J.M.; Verbeek, R.G.F.A. Flexible large-area ultrasound arrays for medical applications made using embossed polymer structures. *Nat Commun* **2024,** *15*, 2802.
26. Dahl, T.; Ealo, J.L.; Bang, H.J.; Holm, S.; Khuri-Yakub, P. Applications of airborne ultrasound in human–computer interaction. *Ultrasonics* **2014**, *54*(7), 1912–1921.
27. Tovar-Lopez, F.J. Recent Progress in Micro- and Nanotechnology-Enabled Sensors for Biomedical and Environmental Challenges. *Sensors* **2023**, *23*, 5406.
28. Carotenuto, R.; Pezzimenti, F.; Della Corte, F.G.; Iero, D.; Merenda, M. Ranging with Frequency Dependent Ultrasound Air Attenuation. *Sensors* **2021**, *21(15)*, 4963.
29. Turo, A.; Salazar, J.; Chavez, J.A.; Kichou, H.B.; Gomez, T.E.; De Espinosa, F.M.; Garcia-Hernandez, M.J. Ultra-low noise front-end electronics for air-coupled ultrasonic non-destructive evaluation. *NDT & E International* **2003**, *36*(2), 93-100.
30. Mehta, A., Vasudev, H. Advances in welding sensing information processing and modelling technology: an overview. *Journal of Adhesion Science and Technology* **2024**, *38(4)*, 1–45.
31. Schmid, S.; Dürrmeier, F.; Grosse, C. Spatial and Temporal Deep Learning in Air-Coupled Ultrasonic Testing for Enabling NDE 4.0. *Journal of Nondestructive Evaluation* **2023**, *42*, 84.
32. Álvarez-Arenas, T.G.; Camacho, J. Air-Coupled and Resonant Pulse-Echo Ultrasonic Technique. *Sensors* **2019**, *19*, 2221.
33. Larsen, O.N.; Radford, C. Acoustic Conditions Affecting Sound Communication in Air and Underwater. In *Effects of Anthropogenic Noise on Animals*; Slabbekoorn, H.; Dooling, R.J.; Popper, A.N.; Fay, R.R., Eds.; Springer: New York, NY, USA, 2018; *Springer Handbook of Auditory Research*, **66**, 109–144.
34. Olisa, S.C.; Khan, M.A.; Starr, A. Review of Current Guided Wave Ultrasonic Testing (GWUT) Limitations and Future Directions. *Sensors* **2021**, *21*, 811.
35. Chen, H.; Sun, Q.; Xuan, L.; Lin, Z.; Yang, Z.; Huang, X.; Li, Z.; Gao, W.; Ren, J.; Shi, J.; Zou, X. Ultrasonic technology for predicting beef thawing degree and endpoint. *Journal of Food Engineering* **2024**, *383*, 112236.
36. Orellana, A.E.M.; Mendler, A.; Schmid, S.; Grosse, C.U. Predictive probability of detection curves for ultrasonic testing. *NDT & E International* **2025**, *153*, 103346.
37. Dardouri, A.; Othmani, C.; Salah, I.B.; Zhang, B.; Njeh, A. Guided waves in sandwich plates: revealing an approximate threshold of contrast material properties for Legendre polynomial method limitations. *Acta Mechanica Sinica* **2025**, *41*(6), 424272.
38. Kachanov, V.K.; Sokolov, I.V.; Karavaev, M.A. Selecting optimum air gap length in air-coupled ultrasonic through-transmission testing of products made of polymer materials. *Russian Journal of Nondestructive Testing* **2025**, *61*(5), 505-516.

 doi:10.20944/preprints202602.0014.v1

39. Boccaccio, M.; Rachiglia, P.; Malfense Fierro, G.P.; Pio Pucillo, G.; Meo, M. Deep-Subwavelength-Optimized Holey-Structured Metamaterial Lens for Nonlinear Air-Coupled Ultrasonic Imaging. *Sensors* **2021**, *21*, 1170.
40. Jeger-Madiot, N.; Gateau, J.; Fink, M.; Ing, R.K. Non-contact and through-clothing measurement of the heart rate using ultrasound vibrocardiography. *Medical Engineering & Physics* **2017**, *50*, 96–102.
41. Jeng, G.S.; Chen, S.; Hsieh, L.T.; Lo, M.T. Contactless Respiratory Waveform Estimation Using Ultrasound Planar Array. *IEEE Open Journal of Ultrasonics, Ferroelectrics, and Frequency Control* **2025**, *5*, 23–32.
42. Ambrosanio, M.; Franceschini, S.; Grassini, G.; Baselice, F. A multi-channel ultrasound system for non-contact heart rate monitoring. *IEEE Sensors Journal* **2020**, *20*(4), 2064–2074.
43. Cailly, W.; Gonzalez-Diaz, R.; Nieminen, H.J Accuracy and robustness of an air-ultrasound method for non-contact heart rate and heart rate variability measurements Open Access. *J. Acoust. Soc. Am.* **2018**, *158*, 2979–2994 .
44. Shahshahani, A.; Zilic, Z.; Bhadra, S. An ultrasound-based biomedical system for continuous cardiopulmonary monitoring: A single sensor for multiple information. *IEEE Transactions on Biomedical Engineering* **2020**, *67*(1), 268–276.
45. Wang, T.; Zhang, D.; Wang, L.; Zheng, Y.; Gu, T.; Dorizzi, B.; Zhou, X. Contactless respiration monitoring using ultrasound signal with off-the-shelf audio devices. *IEEE Internet of Things Journal* **2019**, *6*(2), 2959–2973.
46. Min, S.D.; Kim, J.K.; Shin, H.S.; Yun, Y.H.; Lee, C.K.; Lee, M. Noncontact respiration rate measurement system using an ultrasonic proximity sensor. *IEEE Sensors Journal* **2010**, *10*(11), 1732–1739.
47. Singh, A.; Rehman, S.U.; Yongchareon, S.; Chong, P.H.J. Multi-resident non-contact vital sign monitoring using radar: A review. *IEEE Sensors Journal* **2020**, *21(4)*, 4061–4084.
48. Rehouma, H.; Noumeir, R.; Essouri, S.; Jouvet, P. Advancements in Methods and Camera-Based Sensors for the Quantification of Respiration. *Sensors* **2020**, *20*, 7252.
49. Gatzoulis, L.; Iakovidis, I. Wearable and portable eHealth systems. *IEEE Engineering in Medicine and Biology Magazine* **2007**, *26(5)*, 51-56.
50. Chen, A.; Rhoades, R.D.; Halton, A.J.; Booth, J.C.; Shi, X.; Bu, X.; Wu, N.; Chae, J. Wireless Wearable Ultrasound Sensor to Characterize Respiratory Behavior. *Methods in Molecular Biology* **2022**, *2393*, 671−682.
51. Massaroni, C.; Nicoló, A.; Sacchetti, M.; Schena, E. Contactless methods for measuring respiratory rate: A review. *IEEE Sensors J.* **2021**, *21 (11)*, 12821–12839.
52. Selvaraju, V.; Spicher, N.; Wang, J.; Ganapathy, N.; Warnecke, J.M.; Leonhardt, S.; Swaminathan, R.; Deserno, T.M. Continuous Monitoring of Vital Signs Using Cameras: A Systematic Review. *Sensors* **2022**, *22*, 4097.
53. Moon, H.H.; Lee, G.Y.; Kim, G.S.; Ra, G.L.; Jeong, J.S. Bidirectional non-contact ultrasound imaging using MHz-band air-coupled ultrasound transducer for skin assessment: A feasibility study. *Ultrasonics* **2025**, *161*, 107948.
54. Kawai, K.; Ohara, R.; Sato, S.; Ishii, T.; Izumi, S.; Kawaguchi, H. Contactless respiration measurement system using 25-kHz spatial ultrasound Doppler sensor. *In 2023 IEEE International Ultrasonics Symposium*, Montreal, QC, Canada, 3-8 September 2023.
55. Melo, D.F.; Silva, B.M.; Pombo, N.; Xu, L. Internet of things assisted monitoring using ultrasound-based gesture recognition contactless system. *IEEE Access* **2021**, *9*, 90185-90194.
56. Sgambato, B.G.; Hasbani, M.H.; Barsakcioglu, D.Y.; Ibáñez, J.; Jakob, A.; Fournelle, M.; Tang, M.T.; Farina, D. High performance wearable ultrasound as a human-machine interface for wrist and hand kinematic tracking. *IEEE Transactions on Biomedical Engineering* **2024**, *71*(2), 484–493.
57. Kim, K.; Kim, S.; Choi, A. Ultrasonic Sound Guide System with Eyeglass Device for the Visually Impaired. *Sensors* **2022**, *22*, 3077.
58. Panazan, C.-E.; Dulf, E.-H. Intelligent Cane for Assisting the Visually Impaired. *Technologies* **2024**, *12*, 75.
59. Mikaël A Mousse. Visually Impaired People Monitoring in a Smart Home using Electronic White Cane. *International Journal of Computer Science and Information Technology* **2022**, *14*, 101−110.
60. Bai, J.; Lian, S.; Liu, Z.; Wang, K.; Liu, D. Smart guiding glasses for visually impaired people in indoor environment. *IEEE Transactions on Consumer Electronics* **2017**, 63(3), 258−266.

 doi:10.20944/preprints202602.0014.v1

61. Franceschini, S.; Ambrosanio, M.; Autorino, M. M.; Baselice, F. A Novel Ultrasound System for Contactless Quantitative Measurements of Finger Tapping: A Feasibility Study. *In 2024 IEEE International Conference on E-health Networking, Application & Services (HealthCom)*, Nara, Japan, 2024, 1–5.
62. Sohl-Dickstein, J.; Teng, S.; Gaub, B.M.; Rodgers, C.C.; Li, C.; DeWeese, M.R.; Harper, N.S. A Device for Human Ultrasonic Echolocation. *IEEE Trans Biomed Eng.* **2015**, *62(6)*, 1526–1534.
63. He, K. Ultrasound-based human machine interfaces for hand gesture recognition: A scoping review and future direction. *IEEE Transactions on Medical Robotics and Bionics* **2025**, *7(1)*, 200–212.
64. Huang, Y.; Yang, X.; Li, Y.; Zhou, D.; He, K.; Liu, H. Ultrasound-based sensing models for finger motion classification. *IEEE Journal of Biomedical and Health Informatics* **2018**, *22*(5), 1395-1405.
65. Blum, F.; Jarzynski, J.; Jacobs, L.J. A focused two-dimensional air-coupled ultrasonic array for non-contact generation. *NDT & E International* **2005**, *38*(8), 634–642.
66. Ma, H.; Wang, Z.; Cheng, Z.; He, G.; Feng, T.; Zuo, C.; Qiu, H. Multiscale confocal photoacoustic dermoscopy to evaluate skin health. *Quantitative Imaging in Medicine and Surgery* **2022**, *12*(5), 2696.
67. Salim, M.S.; Abd Malek, M.F.; Heng, R.B.W.; Juni, K.M.; Sabri, N. Capacitive micromachined ultrasonic transducers: Technology and application. *Journal of Medical Ultrasound* **2012**, *20*(1), 8–31.
68. Ji, Y.; Fan, M.; Li, B.; Gao, G.; Jiang, Z. Rapid In Situ Coating of Covered Stents with Highly Tough, Biocompatible Membrane for Emergency Coronary Artery Perforation. *Biomolecules* **2025**, *15*, 1608.
69. Fritze, H. High-temperature bulk acoustic wave sensors. *Measurement Science and Technology* **2010**, *22*(1), 012002.
70. Matko, V.; Milanovič, M. Detection Principles of Temperature Compensated Oscillators with Reactance Influence on Piezoelectric Resonator. *Sensors* **2020**, *20*, 802.
71. Carr, A.R.; Chan, Y.J.; Reuel, N.F. Contact-Free, Passive, electromagnetic resonant sensors for enclosed biomedical applications: A perspective on opportunities and challenges. *ACS Sensors* **2023**, *8*(3), 943–955.
72. Bera, T.K. Bioelectrical impedance methods for noninvasive health monitoring: a review. *Journal of Medical Engineering* **2014**, *2014*(1), 381251.
73. Seeber, B.U.; Kerber, S.; Hafter, E.R. A system to simulate and reproduce audio–visual environments for spatial hearing research. *Hearing Research* **2010**, *260*(1-2), 1-10.
74. Zeqiri, B.; Scholl, W.; Robinson, S.P. Measurement and testing of the acoustic properties of materials: a review. *Metrologia* **2010**, *47*(2), S156.
75. Chen, J.; Zhao, J.; Lin, L.; Sun, X. Truncated Conical PVDF Film Transducer for Air Ultrasound. *IEEE Sensors Journal* **2019**, *19*, 8618–8625.
76. Turner, R.C.; Fuierer, P.A.; Newnham, R.E.; Shrout, T.R. Materials for high temperature acoustic and vibration sensors: A review. *Applied Acoustics* **1994**, *41*(4), 299-324.
77. Drinkwater, B.W.; Wilcox, P.D. Ultrasonic arrays for non-destructive evaluation: A review. *NDT & E International* **2006**, *39*(7), 525-541.
78. Angiulli, G.; Versaci, M.; Burrascano, P.; Laganá, F. A Data-Driven Gaussian Process Regression Model for Concrete Complex Dielectric Permittivity Characterization. *Sensors* **2025**, *25*, 6350.
79. Pratticò, D.; Laganà, F. Infrared Thermographic Signal Analysis of Bioactive Edible Oils Using CNNs for Quality Assessment. *Signals* **2025**, *6*, 38.
80. Wang, Z.; Li, S.; Shen, G. Advanced Sensory Hardware for Intelligent Eye-Machine Interfacing: from Wearables to Bionics. *Advanced Functional Materials* **2025**, *35(37)*, 2503519.
81. Al-Sakaji, B.A.K.; Al-Asheh, S.; Maraqa, M.A. A Review on the Development of an Integer System Coupling Forward Osmosis Membrane and Ultrasound Waves for Water Desalination Processes. *Polymers* **2022**, *14*, 2710.
82. He, B.; Ji, X.; Li, G.; Cheng, B. Key technologies and applications of UAVs in underground space: a review. *IEEE Transactions on Cognitive Communications and Networking* **2024**, *10*(3), 1026-1049.
83. Rathod, V.T. A Review of Electric Impedance Matching Techniques for Piezoelectric Sensors, Actuators and Transducers. *Electronics* **2019**, *8*, 169.
84. Banafaa, M.; Muqaibel, A.H. Tropospheric Ducting: A Comprehensive Review and Machine Learning based Classification Advancements. *IEEE Access* **2025**, *13*, 22510-22534.

85. Gao, R.; Liang, M.; Dong, H.; Luo, X.; Suganthan, P.N. Underwater acoustic signal denoising algorithms: A survey of the state-of-the-art. *IEEE Transactions on Instrumentation and Measurement* **2025**, *74*, 1-18.
86. Liu, M.; Liu, H.; He, X.; Jin, S.; Chen, P.; Xu, M. Research advances on non-line-of-sight imaging technology. *Journal of Shanghai Jiaotong University (Science)* **2025**, *30*(5), 833-854.
87. Pradhan, S.S.; Unnikrishnan, L.; Mohanty, S.; Nayak, S.K. Thermally conducting polymer composites with EMI shielding: a review. *Journal of Electronic Materials* **2020**, *49*(3), 1749-1764.
88. Cai, Y.; Yu, H.; Cheng, L.; Guo, S.; Liu, T.; Chen, D.; Huang, S.; Hu, Z.; Wang, Y.; Zhou, Y. Structure design, surface modification, and application of CNT microwave-absorbing composites. *Advanced Sustainable Systems* **2023**, *7*(12), 2300272.
89. Fekiač, J.J.; Krbata, M.; Kohutiar, M.; Janík, R.; Kakošová, L.; Breznická, A.; Eckert, M.; Mikuš, P. Comprehensive Review: Optimization of Epoxy Composites, Mechanical Properties, & Technological Trends. *Polymers* **2025**, *17*, 271.
90. Šutka, A.; Lapčinskis, L.; He, D.; Kim, H.; Berry, J.D.; Bai, J.; Knite, M.; Ellis, A.V.; Jeong, C.K.; Sherrell, P. C. Engineering polymer interfaces: a review toward controlling triboelectric surface charge. *Advanced Materials Interfaces* **2023**, *10*(26), 2300323.
91. Hiremath, N.; Kumar, V.; Motahari, N.; Shukla, D. An Overview of Acoustic Impedance Measurement Techniques and Future Prospects. *Metrology* **2021**, *1*, 17-38.
92. Pillai, G.; Li, S.S. Piezoelectric MEMS resonators: A review. *IEEE Sensors Journal* **2021**, *21*(11), 12589-12605.
93. Ma, J.; Hu, J.; Li, Z.; Nan, C.W. Recent progress in multiferroic magnetoelectric composites: from bulk to thin films. *Advanced Materials* **2011**, *23*(9), 1062-1087.
94. Zhang, J.; Wang, J.; Zhong, C.; Zhang, Y.; Qiu, Y.; Qin, L. Flexible Electronics: Advancements and Applications of Flexible Piezoelectric Composites in Modern Sensing Technologies. *Micromachines* **2024**, *15*, 982.
95. Nivedhitha, D. M., & Jeyanthi, S. Polyvinylidene fluoride, an advanced futuristic smart polymer material: A comprehensive review. *Polymers for Advanced Technologies* **2023**, *34*(2), 474-505.
96. Fiorillo, A.S.; Pullano, S.A.; Critello, C.D. Spiral-shaped biologically-inspired ultrasonic sensor. *IEEE Transactions on Ultrasonics, Ferroelectrics, and Frequency Control* **2020**, *67*(3), 635-642.
97. Pullano, S.A.; Bianco, M.G.; Critello, D.C.; Menniti, M.; La Gatta, A.; Fiorillo, A.S. A Recursive Algorithm for Indoor Positioning Using Pulse-Echo Ultrasonic Signals. *Sensors* **2020**, *20*, 5042.
98. Müller, R.; Kuc, R. Biosonar-inspired technology: goals, challenges and insights. *Bioinspiration & biomimetics* **2007**, *2*(4), S146.
99. Roy, S.; Azad, A.W.; Baidya, S.; Alam, M.K.; Khan, F. Powering solutions for biomedical sensors and implants inside the human body: A comprehensive review on energy harvesting units, energy storage, and wireless power transfer techniques. *IEEE Transactions on Power Electronics* **2022**, *37*(10), 12237-12263.
100. Wu, T.; You, D.; Gao, H.; Lian, P.; Ma, W.; Zhou, X.; Wang, C.; Luo, J.; Zhang, H.; Tan, H. Research Status and Development Trend of Piezoelectric Accelerometer. *Crystals* **2023**, *13*, 1363.
101. Bibbò, L.; Angiulli, G.; Laganà, F.; Pratticò, D.; Cotroneo, F.; La Foresta, F.; Versaci, M. MEMS and IoT in HAR: Effective Monitoring for the Health of Older People. *Appl. Sci.* **2025**, *15*, 4306.
102. Zhu, J.; Liu, X.; Shi, Q.; He, T.; Sun, Z.; Guo, X.; Liu, W.; Sulaiman, O.B.; Dong, B.; Lee, C. Development Trends and Perspectives of Future Sensors and MEMS/NEMS. *Micromachines* **2020**, *11*, 7.
103. Birjis, Y.; Swaminathan, S.; Nazemi, H.; Raj, G.C.A.; Munirathinam, P.; Abu-Libdeh, A.; Emadi, A. Piezoelectric Micromachined Ultrasonic Transducers (PMUTs): Performance Metrics, Advancements, and Applications. *Sensors* **2022**, *22*, 9151.
104. Wong, S.J.; Roy, K.; Lee, C.; Zhu, Y. Thin-film piezoelectric micromachined ultrasound transducers in biomedical applications: A review. *IEEE Transactions on Ultrasonics, Ferroelectrics, and Frequency Control* **2024**, *71*(6), 622-637.
105. **Svilainis, L.; Dumbrava, V.** Design of a Low-Noise Preamplifier for Ultrasonic Transducers. *Ultragarsas (Ultrasound)* **2005**, *55*, 28–32.
106. **Choi, H.** Design of Preamplifier for Ultrasound Transducers. *Sensors* **2024**, *24*, 786.
107. **Zamora, I.; Ledesma, E.; Uranga, A.; Barniol, N.** Miniaturized 0.13-µm CMOS Front-End Analog for AlN PMUT Arrays. *Sensors* **2020**, *20*, 1205.

108. Olivieri, R.; Barile, G.; Stornelli, V.; Ciarrocchi, D.; Fonte, M.; Zompanti, A.; Ferri, G. A novel current-mode EMG interface. In Proc. Int. Workshop Advances in Sensors and Interfaces (IWASI), Manfredonia, Italy, 2025; 1–6.
109. Ozer, E.; Kacar, F. Current-mode PID controller using second-generation voltage conveyor (VCII). J. Circuits Syst. *Comput.* **2022**, *31(17)*, 2250295.
110. Olivieri, R.; Di Lizio, G.A.; Barile, G.; Stornelli, V.; Ferri, G.; Minaei, S. Conveyor-based single-input triple-output second-order LP/BP and cascaded first-order HP filters. *Electronics* **2025**, *14*, 3514.
111. **Safari, L.; Barile, G.; Stornelli, V.; Ferri, G.** A Review on VCII Applications in Signal Conditioning for Sensors and Bioelectrical Signals: New Opportunities. *Sensors* **2022**, *22*, 3578.
112. **O'Reilly, M.A.; Hynynen, K.** A PVDF Receiver for Ultrasound Monitoring of Transcranial Focused Ultrasound Therapy. *IEEE Transactions on Biomedical Engineering* **2010**, *57*, 2286–2294.
113. **Pullano, S.A.; Fiorillo, A.S.; Barile, G.; Stornelli, V.; Ferri, G.** A Second-Generation Voltage-Conveyor-Based Interface for Ultrasonic PVDF Sensors. *Micromachines* **2021**, *12*, 99.
114. **Barile, G.; Pullano, S.A.; Fiorillo, A.S.; Ferri, G.** A Broadband Approach for the Generation and Reception of Low-Frequency Ultrasounds In-Air for Sonar Applications. In *Proceedings of the 2021 International Conference on e-Health and Bioengineering (EHB)*, Iași, Romania, 18–19 November 2021; 1–4.
115. **Lin, Y.; O'Reilly, M.A.; Hynynen, K.** A PVDF Receiver for Acoustic Monitoring of Microbubble-Mediated Ultrasound Brain Therapy. *Sensors* **2023**, *23*, 1369.
116. Rui, G.; Allahyarov, E.; Zhu, Z.; Huang, Y.; Wongwirat, T.; Zou, Q.; Taylor, P.L.; Zhu, L. Challenges and opportunities in piezoelectric polymers: Effect of oriented amorphous fraction in ferroelectric semicrystalline polymers. *Responsive Materials* **2024**, *2*(3), e20240002.
117. Kashdan, J. T.; Shrimpton, J. S.; Whybrew, A. Two-phase flow characterization by automated digital image analysis. Part 1: fundamental principles and calibration of the technique. *Particle & Particle Systems Characterization: Measurement and Description of Particle Properties and Behavior in Powders and Other Disperse Systems* **2003**, *20*(6), 387-397.
118. Boujenoui, A.; El Atlas, N.; Bybi, A.; Reskal, H.; Elmaimouni, L. Advances in Crosstalk Reduction Techniques for Ultrasonic Transducer Arrays. *Sensors* **2025**, *25*, 7666.
119. Weng, C.; Gu, X.; Jin, H. Coded Excitation for Ultrasonic Testing: A Review. *Sensors* **2024**, *24*, 2167.
120. Zhu, B.; Ma, Y.; Zhou, Z.; Guo, W.; Zhu, J.; Zhu, X. Underwater Acoustic Signal Denoising with Diffusion-based Generative Models. *Signal Processing* **2025**, *242*, 110430.
121. Boris, I.; Barashok, K.; Choi, Y.; Choi, Y.; Aslam, M.; Lee, J. Machine learning techniques in ultrasonics-based defect detection and material characterization: A comprehensive review. *Advances in Mechanical Engineering* **2025**, *17(6)*, 1–41.
122. Yan, J.; Zhang, Y.; Jiao, Z.; Song, L.; Wang, Z.; Zhang, Q.; Liu, Y.; Qin, W. Opportunities and challenges of ultrasonic diagnostic techniques for plant-based food monitoring: Principle, machine system, and application strategies. *Critical Reviews in Food Science and Nutrition* **2025**, *65*(28), 5632-5651.
123. Sethi, A.K.; Muddaloor, P.; Anvekar, P.; Agarwal, J.; Mohan, A.; Singh, M.; Gopalakrishnan, K.; Yadav, A.; Adhikari, A.; Damani, D.; Kulkarni, K.; Aakre, C.A.; Ryu, A.J.; Iyer, V.N.; Arunachalam, S.P.; Digital Pulmonology Practice with Phonopulmography Leveraging Artificial Intelligence: Future Perspectives Using Dual Microwave Acoustic Sensing and Imaging. *Sensors* **2023**, *23*, 5514.
124. Alzahab, N.A.; Apollonio, L.; Di Iorio, A.; Alshalak, M.; Iarlori, S.; Ferracuti, F.; Monteriù, A.; Porcaro, C. Hybrid Deep Learning (hDL)-Based Brain-Computer Interface (BCI) Systems: A Systematic Review. *Brain Sci.* **2021**, *11*, 75.
125. Pullano, S. A.; Oliva, G.; Presta, P.; Carullo, N.; Musolino, M.; Andreucci, M.; Bolignano, D.; Fiorillo, A.S.; Coppolino, G. A portable easy-to-use triboelectric sensor for arteriovenous fistula monitoring in dialysis patients. *Sensors International* **2025**, *6*, 100309.
126. Ramadas C.; Janardhan Padiyar M.; Balasubramaniam K.; Joshi, M.; Krishnamurthy, C.V. Delamination size detection using time of flight of anti-symmetric (Ao) and mode converted Ao mode of guided Lamb waves. *J Intell Mater Syst Struct* **2010**; *21*, 817–825.
127. Fan, Z.; Bai, K.; Chen, C. Ultrasonic testing in the field of engineering joining. *The International Journal of Advanced Manufacturing Technology* **2024**, *132*(9), 4135-4160.

 doi:10.20944/preprints202602.0014.v1

128. Ramaswami, M. Network plasticity in adaptive filtering and behavioral habituation. *Neuron* **2014**, *82*(6), 1216–1229.
129. Mitra, M.; Gopalakrishnan, S. Guided wave based structural health monitoring: A review. *Smart Materials and Structures* **2016**, *25*(5), 053001.
130. Ostrysz, M.; Szczepaniak, Z.; Sondej, T. Non-Contact Measurement of Human Vital Signs in Dynamic Conditions Using Microwave Techniques: A Review. *Sensors* **2026**, *26*, 359.
131. Guo, X.; Zhang, Z.; Ren, Z.; Li, D.; Xu, C.; Wang, L.; Liu, W.; Zhuge, Y.; Zhou, G.; Lee, C. Advances in Intelligent Nano-Micro-Scale Sensors and Actuators: Moving toward Self-Sustained Edge AI Microsystems. *Advanced Materials 2025*, *37*(50), e10417.